Preprints (www.preprints.org) | NOT PEER-REVIEWED | Posted: 14 May 2019 doi:10.20944/preprints201905.0167.v1

Photosynthetic function and the photoprotective mechanism of leaves of *Morus alba* L. seedlings under NaCl and $NaHCO_3$ stress revealed by proteomics

Zhang Hui-hui[1a†], Xu Nan[2,3†], Li Xin[a], Sun Guang-yu[3], Shi Guang-liang[1b*]

1a. College of resources and environment, Northeast Agricultural University, Harbin Heilongjiang, China

1b. College of Veterinary Medicine, Northeast Agricultural University, Harbin Heilongjiang, China

2. Natural Resources and Ecology Institute, Heilongjiang Sciences Academy, Harbin Heilongjiang, China

3. College of life sciences. Northeast Forestry University, Harbin, Heilongjiang, China

4. College of Forestry, Shenyang Agricultural University, Shenyang, China

†Equal contributors

*For correspondence: shiguangliang@neau.edu.cn

Abstract: Photosynthetic function, photoprotection, and the response of related proteomics of mulberry (*Morus alba* L.) seedling leaves under NaCl and $NaHCO_3$ stress with the same Na^+ concentration (100 mmol·L^{-1}) were studied by using photosynthetic gas exchange and chlorophyll fluorescence techniques combined with TMT proteomics. The results showed that NaCl stress had no significant effect on photosystem II (PSII) activity in mulberry seedling leaves, and the expressions of the related proteins, OEE3-1 and PPD4, of the PSII oxygen-evolving complex (OEC) and the antenna proteins, CP24 10A, CP26, and CP29, of LHCII in the leaves also increased to varying degrees. The photosystem I (PSI) activity in the leaves of mulberry seedling also increased, and the expressions of some proteins, PsaF, PsaG, PsaH, PsaL, PsaN, and Ycf4, in PSI increased significantly under NaCl stress. Under $NaHCO_3$ stress, the activity of PSII and PSI and the expression of their protein complexes and the electron transfer-related proteins significantly decreased. NaCl stress had little effect on RuBP regeneration during dark reaction in the leaves and the expressions of glucose synthesis related proteins and net photosynthetic rate (P_n) did not decrease significantly. The leaves could adapt to NaCl stress by reducing stomatal conductance (G_s) to increase water use efficiency (WUE). Under $NaHCO_3$ stress, the expression of dark reaction-related proteins was mostly down-regulated, and G_s was significantly reduced, which indicated that non-stomatal factors were important reasons for the significant inhibition of carbon assimilation. In the photoprotective mechanism under NaCl stress, the expression of cyclic electron flow (CEF) related proteins, ndhH, ndhI, ndhK, and ndhM, involved in NAD(P)H dehydrogenase (NDH) and the key enzyme of the xanthophyll cycle, violaxanthin de-epoxidase (VDE) were up-regulated. In addition, the ratio of xanthophyll cycle components (A+Z)/(V+A+Z) was increased. The expressions of proteins FTR and Fd-NiR, which are related to Fd-dependent ROS metabolism and nitrogen metabolism, were also significant up-regulated under NaCl stress, which can effectively reduce the electronic pressure on Fd. Under $NaHCO_3$ stress, the expressions of CEF-related proteins, VDE, ZE, FTR, Fd-NiR, Fd-GOGAT, SGAT, and GGAT, were significant down-regulated, and the photoprotective mechanism, like the xanthophyll cycle, CEF, and photorespiration, might be damaged, resulting in the inhibition of PSII activity and carbon assimilation in leaves of mulberry seedling under $NaHCO_3$ stress.

Keywords: *Morus alba* L., Salinity, Alkalinity, Proteomics, Photosynthesis, Photoprotective mechanism

Soil salinization is one of the important factors affecting plant growth and distribution. Approximately 20% of arable land and 50% of irrigated land is affected by soil salinization to varying degrees (Zhu et al., 2001; Bhatnagar-Mathur et al., 2008), which seriously threatens food security and the stability of natural ecosystems (Peng et al., 2008). Normal salt content plays an important role in maintaining normal physiological functions of plants, but excessive salt in soil causes osmotic stress (Munns and James, 2006), ion toxicity (Parida and Das, 2005) and disturbance of nutrient ion balance (Yan et al., 2006; Akita and Cabusla, 2000), thus affecting plant growth and physiological functions (Greenway and Munns, 1980; Forni et al., 2017). In the natural environment, the salts in soil are mainly neutral salts, like NaCl and $NaSO_4$, and alkaline salts, such as Na_2CO_3 and $NaHCO_3$ (Yang et al., 2007). However, in China, the main salts in soil are NaCl in coastal areas and $NaHCO_3$ in the Songnen Plain, Northeast China. Different types of salt stress have different effects on plant growth and physiological characteristics. At present, many studies have shown that the damage of alkaline salts, mainly $NaHCO_3$ and Na_2CO_3, to plants is much greater than that of neutral salts (Pang et al., 2016; Campbell et al., 2000, Zhang et al., 2009), which is due to the fact that under alkaline stress, plants have to withstand the same osmotic stress and ion toxicity as salt stress, as well as high pH stress (Guo et al., 2015; Li et al., 2010; Song et al., 2017).

Photosynthesis is the basis of ensuring the normal growth and development of plants under stress. Saline-alkali stress could

affect chlorophyll synthesis and photosynthetic capacity of plants, thus resulting in the decrease of the activity of the photosystem II (PSII) reaction center, the blockage of electron transport, and the limitation of carbon assimilation (Guo et al., 2013; Gong et al., 2013; Mitsuya et al., 2000), but plants also have evolved a series of photoprotective mechanisms under stress, such as the rapid turnover of D1 protein (Yang et al., 2014), cyclic electron flow (CEF) around photosystem I (PSI) (Huang et al., 2018; Zhang et al., 2018a; Huang et al., 2017), photorespiration (Sunil et al., 2018; Messant et al., 2018), and the xanthophyll cycle (Ruban et al., 2010; Gilmore et al., 1996; Pieters et al., 2003). Photosynthesis, especially the photoinhibition of PSII and PSI, is closely related to the production of reactive oxygen species (ROS). Effective removal of photosynthesis-mediated ROS in chloroplasts plays an important role in improving plant stress resistance. Under stress, plants often remove excessive ROS by increasing the activity of antioxidant enzymes (SOD, POD, CAT, APX, and GPX) (Guan et al., 2010; Wu et al., 2012) and the content of antioxidants (ASA and GSH) (Chao et al., 2010; Nie et al., 2007).

The leaves of mulberry (*Morus alba* L.) can be used as silkworm feed, while its fruits can be eaten or brewed because of its rich anthocyanins and vitamins. In addition, mulberry has strong resistance to drought and low temperatures, which makes it an excellent tree species for sand fixation and soil and water conservation, in addition to its economic importance. Recently, mulberry planting and silkworm rearing has been used for the ecological restoration of land in the Songnen Plain of China that has high salinity and is poor for farming. In our previous studies, mulberry was shown to be tolerant to neutral salts but sensitive to alkaline salts, mainly $NaHCO_3$ and Na_2CO_3. Especially under alkaline salt stress, the photosynthetic apparatus is significantly inhibited (Zhang et al., 2012a), yet the reasons are unknown. Under stress, the damage to the photosynthetic apparatus and photoprotective mechanism are related to the protein expression in chloroplasts, but there are few studies on the photosynthesis process and related protein expression of mulberry seedling leaves under NaCl and $NaHCO_3$ stress. Therefore, based on our previous studies, this experiment used proteomics technology combined with photosynthetic gas exchange and chlorophyll fluorescence dynamics technology to study PSII and PSI photochemical activity, photosynthetic carbon assimilation, the photoprotective mechanism, and the response of related proteins under NaCl and $NaHCO_3$ stress with the same Na^+ concentration (100 mmol·L^{-1}) to reveal the response and adaptation mechanism of photosynthesis of the leaves of mulberry seedling to saline-alkali stress. In addition, this study provides basic data for mulberry planting in saline-alkali areas.

1 Materials and methods

1.1 Test materials and treatment

Mulberry seeds were provided by the Silkworm Research Institute of Heilongjiang Academy of Agricultural Sciences. The tested materials were annual mulberry seedlings with a height of approximately 30 cm. Two seedlings were planted in each pot with a diameter of 30 cm and a height of 28 cm, and covered with the substrates of fully mixed peat soil and perlite (v:v=1:1). A total of 15 pots of mulberry seedlings with relatively identical growth were divided into three treatments, with five repeats in each treatment, and treated with 100 mmol·L^{-1} NaCl and $NaHCO_3$ solutions, respectively. Each pot was irrigated with 1 L of NaCl and $NaHCO_3$ solution, and a plastic tray was placed under each pot to prevent the loss of salt solution. The solution flowing into the tray was poured back when the substrate was slightly dry. The same volume of distilled water was irrigated as a control (CK). On the 7th d after irrigation with different saline-alkali solutions, the differences of plants under different treatments were observed and this data was used to calculate the following indexes.

1.2 Determination of parameters and methods

1.2.1 Determination of photosynthetic and physiological indexes

Determination of chlorophyll fluorescence parameters: using dark adaptation clips, the unfolded penultimate leaves treated with different treatments were placed in the dark for 30 min to conduct dark adaptation, and the initial fluorescence (F_o) and maximum fluorescence (F_m) of leaves of mulberry seedling were then measured using a FMS-2 portable modulated fluorometer (Hansatch, UK). The maximum fluorescence (F_m'), minimum fluorescence (F_o'), and steady-state fluorescence (F_s) were measured after light adaptation to calculate the photochemical quenching coefficient (q_P) and non-photochemical quenching (NPQ), where $q_P=(F_m'-F_s)/(F_m'-F_o')$ and $NPQ=(F_s/F_m')-(F_s/F_m)$, respectively. Then, the excess excitation energy $(1-q_P)/NPQ$ of the PS II reaction

center was calculated (Hu et al., 2007). All determinations were repeated three times.

Determination of chlorophyll fluorescence induction curve (OJIP) and 820 optical reflection curve (MR820): the dark adaptation was conducted on unfolded penultimate leaves treated with different treatments for 0.5 h using dark adaptation clips. The OJIP and MR820 curves of leaves were simultaneously measured by M-PEA multi-function plant efficiency analyzer (Hansatch, UK), and the excitation light was induced by pulsed red light (3,000 $\mu mol \cdot m^{-2} \cdot s^{-1}$) provided by the instrument. Each treatment was repeated five times, and the OJIP and MR820 curves were plotted using the average values of five repetitions.

The O, J, I, and P points in the OJIP curve correspond to the time points of 0.01, 2, 30, and 1000 ms, respectively, and their relative fluorescence intensities are expressed by F_o, F_J, F_I, and F_m, respectively. Relative variable fluorescence V_J, V_K, and V_L at 2 ms (J point), 0.3 ms (K point), and 0.15 ms (L point) were obtained on the $V_{O\text{-}P}$ and $V_{O\text{-}J}$ curves standardized by OJIP curves according to $V_{O\text{-}P}=(F_t-F_o)/(F_m-F_o)$, $V_{O\text{-}J}=(F_t-F_o)/(F_J-F_o)$, and $V_{O\text{-}K}=(F_t-F_o)/(F_K-F_o)$. According to Strasser *et al.* (1995), the OJIP curve was analyzed by a JIP-test to obtain PSII maximum photochemical efficiency (F_v/F_m), the photosynthesis indices based on the absorption of light energy (PI_{ABS}), and the total performance index (PI_{total}).

The activity of the PSI reaction center is reflected by the slope ($\triangle I/I_o$) of the initial section of the MR820 curve, where I_o and $\triangle I$ represent the maximum value and the difference between maximum and minimum values of the reflected signal on the MR820 curve, respectively(Oukarroum et al., 2013).

Determination of photosynthetic gas exchange parameters: The unfolded penultimate leaves of mulberry seedling in different treatments were selected and detected under the conditions of 400 $\mu l \cdot L^{-1}$ fixed CO_2 by a CO_2 cylinder and 1,000 $\mu mol \cdot m^{-2} \cdot s^{-1}$ light intensity PFD setting by a built-in light source. The parameters of net photosynthetic rate (P_n), stomatal conductance (G_s), and transpiration rate (T_r) under different treatments were measured, and the instantaneous water use efficiency (WUE) of leaves was further calculated using the equation $WUE=P_n/T_r$. The test was repeated five times.

Extraction and determination of xanthophyll components: The whole process of extracting pigments was conducted in the dark. Leaves (0.2 g) were placed in a pre-cooled mortar and ground until homogenous with 4 mL 85% acetone and SiO_2. After adding another 1 mL 100% acetone and homogenizing for 1 min, the sample was placed on ice for 15 min, then centrifuged for 2 min at 1,200×*g*. Then, the supernatant was removed and filtered through a 0.45 μm microporous membrane filter. The contents of violaxanthin (V), antheraxanthin (A), and zeaxanthin (Z) in the xanthophyll cycle were determined by high-performance liquid chromatography, in which the chromatographic column was Spherisorb C18 (5 μm, 250 mm×4.6 mm), the liquid A in the mobile phase was acetonitrile and methanol (v:v=85:15), and liquid B was methanol and ethyl acetate (v:v=68:32). The flow rate was 1 $mL \cdot min^{-1}$ and the detection wavelength was 445 nm. The deep oxidation state of xanthophyll was expressed by (A+Z)/(V+A+Z).

1.2.2 Proteomic determination and analysis

The leaves of mulberry seedlings in different treatments were collected and pre-cooled with liquid nitrogen, and then sent to PTM Biolabs in Hangzhou Eco & Tech Developmental Area (Hangzhou, Zhejiang Province) in an incubator with dry ice for proteomic determination. The operations were as follows:

(1) Protein extraction: Samples stored at -80 °C were weighed, and then placed in a liquid nitrogen pre-cooled mortar and ground to powder by adding liquid nitrogen. The samples from each treatment were subjected to ultrasonic pyrolysis with phenol extraction buffer (10 $mmol \cdot L^{-1}$ dithiothreitol, 1% protease inhibitor, and 2 $mmol \cdot L^{-1}$ EDTA) at four times the volume of sample powder. An equal volume of tris-saturated phenol was added to the sample. After centrifugation for 10 min at 4 °C and 5,500 g, the supernatant was removed. Five times volume of 0.1 M ammonium acetate/methanol was added for overnight precipitation. The protein precipitation was washed with methanol and acetone, respectively. Finally, the precipitation was re-dissolved with 8 M urea, and the protein concentration was determined using a BCA kit.

(2) Trypsin hydrolysis: After adding dithiothreitol to adjust the final concentration of the protein solution to 5 $mmol \cdot L^{-1}$, the solution was reduced at 56 °C for 30 min. Then, iodoacetamide was added to the solution to adjust its final concentration to 11 $mmol \cdot L^{-1}$, and the solution was incubated at room temperature for 15 min. After the urea concentration of samples was diluted to less than 2 M, trypsin was added in the protein solution with the mass ratio of 1:50 (trypsin: protein) and enzymatic hydrolysis was carried out overnight at 37 °C. Trypsin was added again with the mass ratio of 1:100 (trypsin: protein) and enzymatic hydrolysis continued for another 4 h.

(3) TMT marker: After desalination with Strata X C18 (Phenomenex), the trypsin-hydrolyzed peptide segments were

freeze-dried in a vacuum. After dissolving with 0.5 M TEAB, the peptide segment was labeled according to the instructions provided with the TMT kit. Briefly, the steps were as follows: the label reagent was dissolved in acetonitrile after thawing, mixed with the peptide segment, and incubated at room temperature for 2 h. Then the labeled peptide segment was freeze-dried in a vacuum after desalination.

(4) HPLC classification: Peptide segments were classified by high pH reverse HPLC with the chromatographic column of Agilent 300 Extend C18 (5 μm diameter, 4.6 mm inner diameter, and 250 mm long). The operation was as follows: the gradient of peptide segments was 8%–32% acetonitrile with pH 9, and 60 components were separated in 60 min, then the peptide segments were merged into nine components. The merged components were vacuum freeze-dried for subsequent operations.

(5) Liquid chromatography–mass spectrometry (LC–MS): The peptide segments were dissolved by the liquid chromatography mobile phase A (0.1% (v/v) formic acid aqueous solution), and then separated by an EASY-nLC 1000 Liquid Chromatography System. The mobile phase A was an aqueous solution containing 0.1% formic acid and 2% acetonitrile, and the mobile phase B was an aqueous solution containing 0.1% formic acid and 90% acetonitrile. The liquid phase gradient was set as follows: 0~50 min, 7%–16% B; 50~85 min, 16%–30% B; 85~87 min, 30%–80% B; 87~90 min, 80% B, and the flow rate was maintained at 400 nL/min.

After separation by an EASY-nLC 1000 Liquid Chromatography System, peptide segments were injected into the NSI ion source for ionization, and then analyzed by Orbitrap Lumos™ mass spectrometry. The voltage of ion source was set to 2.0 kV, and the parent ions of peptide segments and their secondary fragments were detected and analyzed by high resolution Orbitrap. The scanning range of MS1 scan was set to 350–1,550 m/z and the scanning resolution was 60,000, while that of MS2 scan was set to 100 m/z with the scanning resolution of 30,000. The data-dependent acquisition (DDA) mode was used to collect data, that is, after the MS1 scan, the first 20 peptide parent ions with the highest signal intensity were selected to enter the HCD collision pool in turn, and fragmented with 32% fragmentation energy. Similarly, the MS2 scan was carried out in turn. To improve the effective utilization of mass spectrometry, automatic gain control (AGC) was set to 5E4, the signal threshold was set to 50,000 ions/s, maximum injection time was set to 70 ms, and the dynamic elimination time of tandem mass spectrometry scanning was set to 30 s to avoid repeated scanning of parent ions.

(6) Database search: MS2 data were retrieved using Maxquant (v1.5.2.8). The retrieval parameters were set as follows: UniProt Morus (27,832 sequences) was used as the database, and anti-database was added to calculate the false positive rate (FPR) caused by random matching. The common contamination database was also added to eliminate the influence of contaminated proteins in the identification results. The digestion mode was Trypsin/P, the number of missing sites was two, the minimum length of the peptide segment was 7 amino acid residues, and the maximum modification number of the peptide segment was five. The mass error tolerance of the primary parent ions of the first search and main search was set at 20 ppm and 5 ppm, respectively, and that of the secondary fragment ions was 0.02 Da. Alkylation of cysteine was set as fixed modification, while oxidation of methionine and acetylation of N-terminal proteins were set as variable modification. The quantitative method used TMT-10plex, and the FDR of protein identification and PSM identification was set to 1%. Proteomics methods were repeated three times.

1.3 Data processing

Excel and SPSS (22.0) were used to analyze the measured data. All data were the mean ± standard error (SE) of three repetitions, and the differences among different treatments were compared by one-way ANOVA and LSD.

2 Results

2.1 PSII response center activity and related proteins in leaves of mulberry seedling under NaCl and $NaHCO_3$ stress

As shown in Fig. 1-A, under NaCl stress, the relative fluorescence intensity F_o of leaves of mulberry seedlings at O point did not change significantly compared with CK, but the relative fluorescence intensities F_J, F_I, and F_P at J, I, and P points, respectively, decreased in varying degrees, especially F_P. Under $NaHCO_3$ stress, F_o increased significantly compared with CK, F_J varied insignificantly, F_I and F_P showed a decreasing trend, and the reduction of F_P under $NaHCO_3$ stress was greater than that under NaCl treatment. After defining the relative fluorescence intensity of P, J, and K points as 1 and O point as 0, the original OJIP curve was

standardized according to O-P, O-J, and O-K (Fig. 1-B, Fig. 1-C, and Fig. 1-D, respectively). Under NaCl stress, the standardized O-P, O-J, and O-K curves changed slightly compared with CK. However, under $NaHCO_3$ stress, the relative variable fluorescence V_J of point J at 2 ms on the standardized O-P curve, V_K of point K at 0.3 ms on the standardized O-J curve, and V_L of point L at 0.15 ms on the standardized O-K curve all increased.

Quantitative analysis of V_J, V_K, and V_L changes showed that there was no significant difference between V_J, V_K, V_L, and CK under NaCl stress, but under $NaHCO_3$ stress, they increased by 23.39% (P<0.01), 13.16% (P<0.01), and 15.49% (P<0.01) compared with CK, respectively (Fig. 2).

Fig. 3 revealed that compared with CK, F_v/F_m, PI_{ABS}, and PI_{total} showed insignificant differences under NaCl stress, but they decreased by 18.20% (P<0.01), 73.22% (P<0.01), and 70.56% (P<0.01), respectively, under $NaHCO_3$ stress. The reduction of PI_{ABS} and PI_{total} was obviously greater than that of F_v/F_m.

Under NaCl stress, the comparison with CK (Tab. 1) showed that the expression of D1 and CP47 proteins decreased by 4.58% (P<0.05) and 8.09% (P<0.01), respectively. The expression of CP43 protein did not change significantly, but the expression of D2 protein increased by 5.16% (P<0.01). The expression of chlorophyll a-b binding proteins, such as CP24 10A, CP26, and CP29, were also increased to varying degrees compared with the CK. The expression of PsbE increased by 28.14% compared with CK (P<0.01), but that of PsbH decreased. Under $NaHCO_3$ stress, the expression of the above core protein and chlorophyll a-b binding protein in the PSII reaction were significantly lower than that of CK.

In terms of the donor side of PSII, under NaCl stress, the expression of OEE 1 and OEE2 proteins decreased by 12.25% (P<0.01) and 11.53% (P<0.01), respectively, compared with CK, and that of PPL 1 and PPD3 proteins varied insignificantly. The expression of OEE3-1 and PPD4 proteins increased by 84.22% (P<0.01) and 39.48% (P<0.01), respectively. However, under $NaHCO_3$ stress, the expression of OEE, PsbP-like protein, and PSBP domain-containing protein were significantly lower than CK, except that the expression of PPD4 protein was significantly higher than CK.

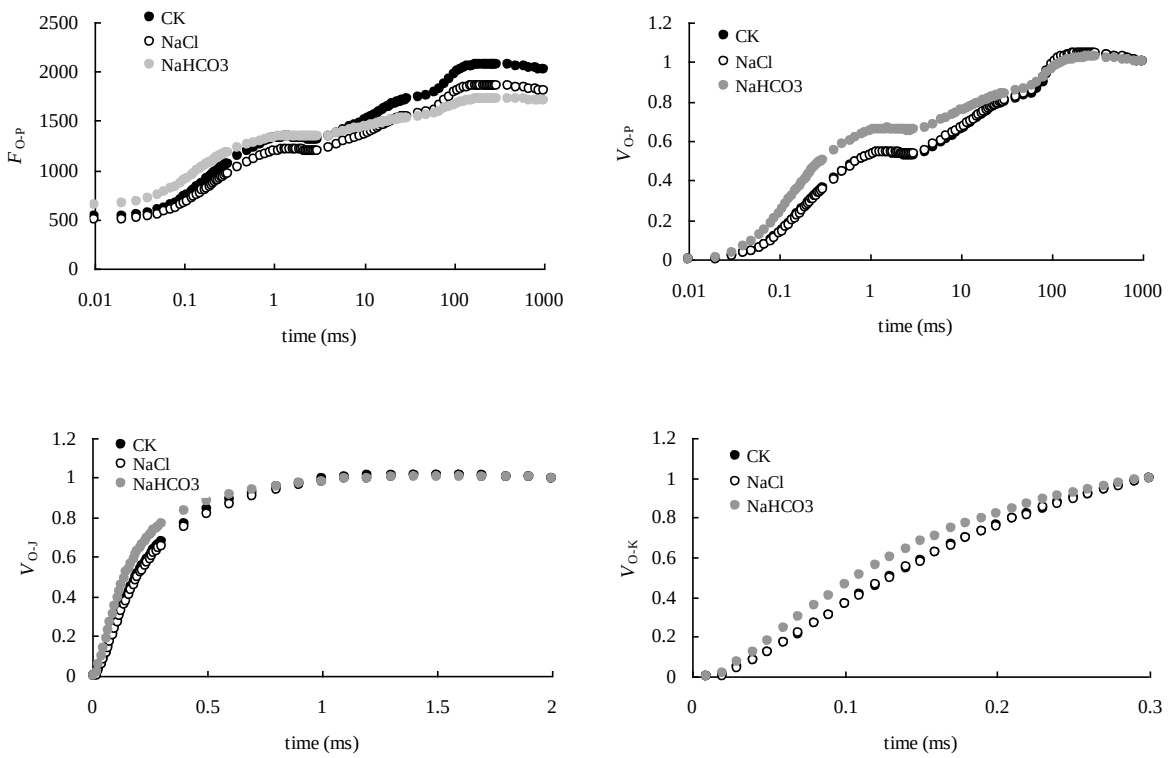

Fig. 1 OJIP curves (A) and standardized O-P, O-J, and O-K curves (B, C and D) of mulberry seedling leaves under NaCl and $NaHCO_3$ stress

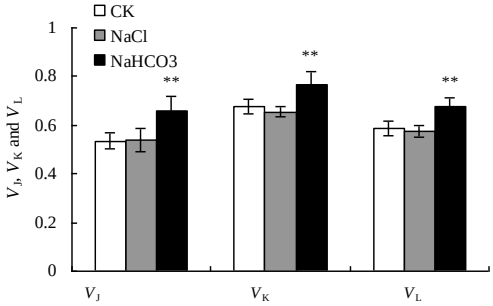

Fig. 2 V_J, V_K, and V_L of mulberry seedling leaves under NaCl and $NaHCO_3$ stress

Note: * represents significant difference with CK (P<0.05), and ** represents very significant difference with CK (P<0.01).

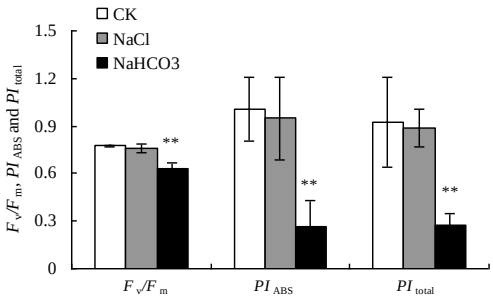

Fig. 3 F_v/F_m, PI_{ABS}, and PI_{total} of mulberry seedling leaves under NaCl and $NaHCO_3$ stress

Note: * represents significant difference with CK (P<0.05), and ** represents very significant difference with CK (P<0.01).

Tab. 1 Expression of PSII response center-related proteins in mulberry seedling leaves under NaCl and $NaHCO_3$ stress

Protein accession	Protein description	Species	Gene name	MW [kDa]	Score	CK	T1	T2
Q09X37	Photosystem II protein D1(D1)	*Morus indica*	psbA	38.892	26.3	1.21±0.01aA	1.15±0.02bA	0.74±0.01cB
Q09X22	Photosystem II D2 protein(D2)	*Morus indica*	PsbD	50.633	323.31	1.14±0.03bA	1.20±0.02aA	0.73±0.01cB
W9QJH4	Photosystem II CP47 reaction center protein(CP47)	*Morus notabilis*	PsbB	51.821	323.31	1.23±0.01aA	1.13±0.03bB	0.73±0.01cC
Q09X21	Photosystem II CP43 reaction center protein (CP43)	*Morus indica*	PsbC	39.577	323.31	1.19±0.01aA	1.18±0.02aA	0.72±0.03bB
W9SBB4	Chlorophyll a-b binding protein CP24 10A (CP24 10A)	*Morus notabilis*	L484_024124	27.454	134.42	0.96±0.04bB	1.56±0.03aA	0.60±0.07cC
W9S9S7	Chlorophyll a-b binding protein CP26 (CP26)	*Morus notabilis*	L484_012656	39.279	230.98	1.01±0.00bB	1.44±0.01aA	0.63±0.04cC
W9QYC0	Chlorophyll a-b binding protein CP29 (CP29)	*Morus notabilis*	L484_026409	30.547	228.16	1.19±0.00bA	1.27±0.05aA	0.65±0.01cB
Q09X00	Cytochrome b559 subunit Alpha (PsbE)	*Morus indica*	PsbE	9.3965	7.6022	1.05±0.03bB	1.34±0.04aA	0.68±0.02cC
Q09WY8	Photosystem II reaction center protein H (PsbH)	*Morus indica*	psbH	7.7489	40.425	1.49±0.02aA	1.13±0.03bB	0.53±0.05cC
W9RXA8	Oxygen-evolving enhancer protein 1 (OEE1)	*Morus notabilis*	L484_011742	35.05	102.58	1.25±0.02aA	1.10±0.01bB	0.74±0.02cC
W9RF48	Oxygen-evolving enhancer protein 2 (OEE2)	*Morus notabilis*	L484_013312	28.333	323.31	1.21±0.01aA	1.07±0.01bB	0.78±0.02cC
W9QQM8	Oxygen-evolving enhancer protein 3-1 (OEE3-1)	*Morus notabilis*	L484_021171	25.249	15.527	0.85±0.00bB	1.56±0.03aA	0.67±0.03cC
W9SDI8	PsbP-like protein 1 (PPL1)	*Morus notabilis*	L484_013529	33.623	2.2618	1.21±0.21aA	1.37±0.18aA	0.55±0.04bB
W9QWE9	PsbP domain-containing protein 3 (PPD3)	*Morus notabilis*	L484_024806	34.31	25.532	1.09±0.02aA	1.07±0.02aA	0.90±0.05bB
W9S5T8	PsbP domain-containing protein 4 (PPD4)	*Morus notabilis*	L484_001712	29.489	45.283	0.80±0.02bB	1.12±0.06aA	1.10±0.09aA

Note: significant differences were expressed by different small letters (P<0.05), and very significant differences were expressed by different capital letters (P<0.01).

2.2 Changes of PSI response center activity and related protein expression in leaves of mulberry seedlings under NaCl and $NaHCO_3$ stress

Compared with CK, the shape of the MR820 curve of leaves of mulberry seedlings changed significantly under NaCl and $NaHCO_3$ stress (Fig. 4-A). The amplitude of the MR820 curve was larger than CK under NaCl stress, but it significantly reduced under $NaHCO_3$ stress. Quantitative analysis of the relative drop ($\triangle I/I_o$) of the MR820 curve in Fig. 4-B showed that under NaCl

stress, $\triangle I/I_o$ increased by 15.68% (P<0.01) compared with CK, while it decreased by 24.09% (P<0.01) under $NaHCO_3$ stress.

As shown in Tab. 2, the expression of psaA, psaB, psaC, psaD, and psaE under NaCl stress was lower than the expression of these proteins in CK. The expression of these proteins also showed a decreasing trend under $NaHCO_3$ stress, and this decrease was significantly greater than that under NaCl treatment. Under NaCl stress, the expression of psaF, psaG, psaH, psaL, psaN, and Ycf4 increased compared with CK. Except for the not significant difference between PsaL and CK, the expression of the other proteins was very significantly different from CK. However, under $NaHCO_3$ stress, the expression of these proteins was significantly lower than CK.

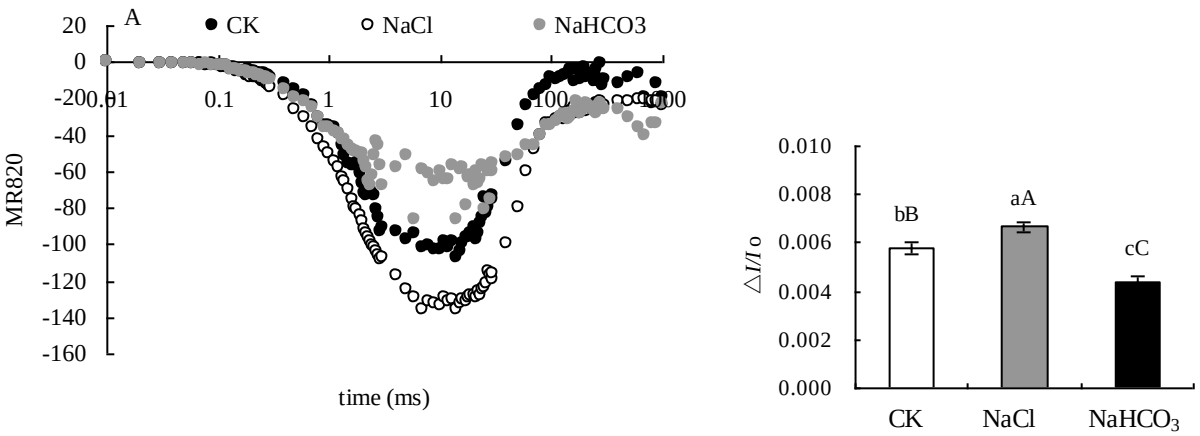

Fig. 4 Reflective fluorescence curve at 820 nm (A) and relative drop ($\triangle I/I_o$) of optical signal at 820 nm of leaves of mulberry seedlings under NaCl and $NaHCO_3$ stress (B)

Tab. 2 Expression of PSI response center related proteins in leaves of mulberry seedlings under NaCl and $NaHCO_3$ stress

Protein accession	Protein description	Species	Gene name	MW [kDa]	Score	CK	T1	T2
Q09X17	Photosystem I P700 chlorophyll a apoprotein A1 (psaA)	*Morus indica*	psaA	83.11	74.698	1.37±0.01aA	1.11±0.03bB	0.64±0.02cC
Q09X18	Photosystem I P700 chlorophyll a apoprotein A2 (psaB)	*Morus indica*	psaB	82.384	82.384	1.24±0.01aA	1.10±0.03bB	0.76±0.01cC
Q09WW7	Photosystem I iron-sulfur center (psaC)	*Morus indica*	PsaC	9.0384	170.06	1.21±0.00aA	1.14±0.02bB	0.71±0.03cC
W9S926	Photosystem I reaction center subunit II (psaD)	*Morus notabilis*	PsaD	23.512	215.05	1.19±0.01aA	1.12±0.01bA	0.75±0.03cB
D3KE88	Photosystem I psaE (psaE)	*Morus alba*	PsaE	15.38	323.31	1.17±0.01aA	1.13±0.02bA	0.76±0.02cB
W9R7D8	Photosystem I reaction center subunit III (psaF)	*Morus notabilis*	PsaF	24.726	151.47	1.01±0.02bB	1.46±0.05aA	0.62±0.02cC
W9QR60	Photosystem I reaction center subunit V (psaG)	*Morus notabilis*	PsaG	17.422	61.803	1.05±0.01bA	1.22±0.04aA	0.79±0.03cC
W9R6H7	Photosystem I reaction center subunit VI (psaH)	*Morus notabilis*	PsaH	15.146	5.0519	1.09±0.05bB	1.26±0.04aA	0.75±0.03cC
W9SVH5	Photosystem I reaction center subunit XI (psaL)	*Morus notabilis*	PsaL	23.137	34.327	1.10±0.04aA	1.16±0.02aA	0.79±0.04bB
W9QUC7	Photosystem I reaction center subunit N (psaN)	*Morus notabilis*	PsaN	18.288	191.75	1.04±0.01bB	1.50±0.08aA	0.57±0.01cC
Q09X06	Photosystem I assembly protein Ycf4 (Ycf4)	*Morus indica*	ycf4	21.306	5.2586	1.21±0.07bB	1.51±0.02aA	0.43±0.02cC

Note: significant differences were expressed by different small letters (P<0.05), and very significant differences were expressed by different capital letters (P<0.01).

2.3 Photosynthetic electron transport and ATP synthase related protein in leaves of mulberry seedlings under NaCl and $NaHCO_3$ stress

The results in Tab. 3 showed that the petA and petC protein expression in the Cyt b6f complex was 8.83% (P<0.05) and 8.66% (P<0.01) lower than CK under NaCl stress, respectively, while that of petB protein increased by 31.99% (P<0.01). Among the other electron transfer related proteins, the expression of Fd and FNR was very significantly reduced, but that of PC was not significantly different compared with CK. Under $NaHCO_3$ stress, the expression of the above electron transfer related proteins was very significantly lower than CK, and the reduction was obviously greater than that of the NaCl treatment. Under NaCl stress, the expression of atpA and atpB in leaves of mulberry seedlings increased by 15.39% (P<0.01) and 7.57% (P<0.01), respectively,

Preprints (www.preprints.org) | NOT PEER-REVIEWED | Posted: 14 May 2019 doi:10.20944/preprints201905.0167.v1

compared with CK, but their expressions under $NaHCO_3$ stress decreased very significantly.

Tab. 3 Photosynthetic electron transport and ATP synthesis-related protein expression in mulberry seedling leaves under NaCl and $NaHCO_3$ stress

Protein accession	Protein description	Species	Gene name	MW [kDa]	Score	CK	T1	T2
Q09X04	Cytochrome f (Cyt f or petA)	*Morus indica*	petA	35.325	323.31	1.15±0.02aA	1.05±0.02bA	0.82±0.04cB
Q09WY7	Cytochrome b6 (Cyt b6 or petB)	*Morus indica*	petB	24.224	32.824	1.02±0.06bB	1.35±0.05aA	0.73±0.05cC
W9R0C1	Cytochrome b6-f complex iron-sulfur subunit (PetC)	*Morus notabilis*	PetC	24.376	219.71	1.23±0.01aA	1.12±0.04bB	0.71±0.01cC
W9RC20	Plastocyanin (PC or PetE)	*Morus notabilis*	PetE	16.574	225	1.16±0.00aA	1.09±0.03aA	0.74±0.03bB
W9R8L4	Ferredoxin (Fd or FetF)	*Morus notabilis*	FetF	15.765	111.2	1.62±0.01aA	1.17±0.03bB	0.39±0.04cC
W9SCQ6	Ferredoxin--NADP reductase (FNR or PetH)	*Morus notabilis*	PetH	39.931	323.31	1.30±0.05aA	1.21±0.02bB	0.60±0.01cC
Q09X32	ATP synthase subunit alpha (atpA)	*Morus indica*	atpA	55.441	323.31	1.09±0.00bB	1.26±0.02aA	0.73±0.01cC
A0A1V0J178	ATP synthase subunit beta (atpB)	*Morus australis*	atpB	53.733	323.31	1.11±0.03bB	1.19±0.00aA	0.77±0.02cC

Note: significant differences were expressed by different small letters (P<0.05), and very significant differences were expressed by different capital letters (P<0.01).

2.4 Photosynthetic gas exchange parameters and carbon assimilation related proteins in leaves of mulberry seedlings under NaCl and $NaHCO_3$ stress

The findings in Fig. 5 showed that P_n did not vary significantly under NaCl stress, but G_s and T_r decreased by 21.31% (P<0.05) and 24.35% (P<0.05), respectively. P_n, G_s and T_r reduced very significantly under $NaHCO_3$ stress. Under NaCl stress, C_i was slightly lower than CK but this difference was not significant (P<0.05). WUE increased by 31.29% (P<0.01) under NaCl stress, while C_i increased significantly under $NaHCO_3$ stress, but WUE did not show much variation.

As shown in Tab. 4, RbcL (Fragment) (R4I779, O20258, Q32625, and U3GQJ9), RbcM (W9RUU9), RCA (Fragment) (A8QIH7), RCA1(W9S2F0), RCA2 (W9RCR8), and RBCMT (W9QMR3) of key enzymes (ribulose-1,5-bisphosphate carboxylase/oxygenase (Rubisco)) of carbon assimilation under NaCl stress did not change significantly. RBCMT (W9QMR3) increased evidently, but under $NaHCO_3$ stress, the expression of above the enzymes and their related subunits all significantly decreased. The differential proteins PGK (W9R524 and W9QWX1) and R5PI (W9RQW9) identified during RuBP regeneration were significantly up-regulated under NaCl stress, and GAPD (W9RTC6, A0A1S6PVK8, W9R0D7, W9R8N5, and W9QWT8), TPI (W9R6S4), SBPase (W9REN5), and TK (W9RGS5) did not change significantly. The key enzymes SBPase (W9REN5 and A8DUA7) in the process of glucose synthesis also did not change significantly. However, besides the up-regulated expression of PGK (W9QWX1), GAPD (W9RTC6, A0A1S6PVK8, and W9R0D7), and R5PI (W9RQW9) under $NaHCO_3$ stress, the expression of other proteins identified in dark reactions was significantly down-regulated.

Preprints (www.preprints.org) | NOT PEER-REVIEWED | Posted: 14 May 2019 doi:10.20944/preprints201905.0167.v1

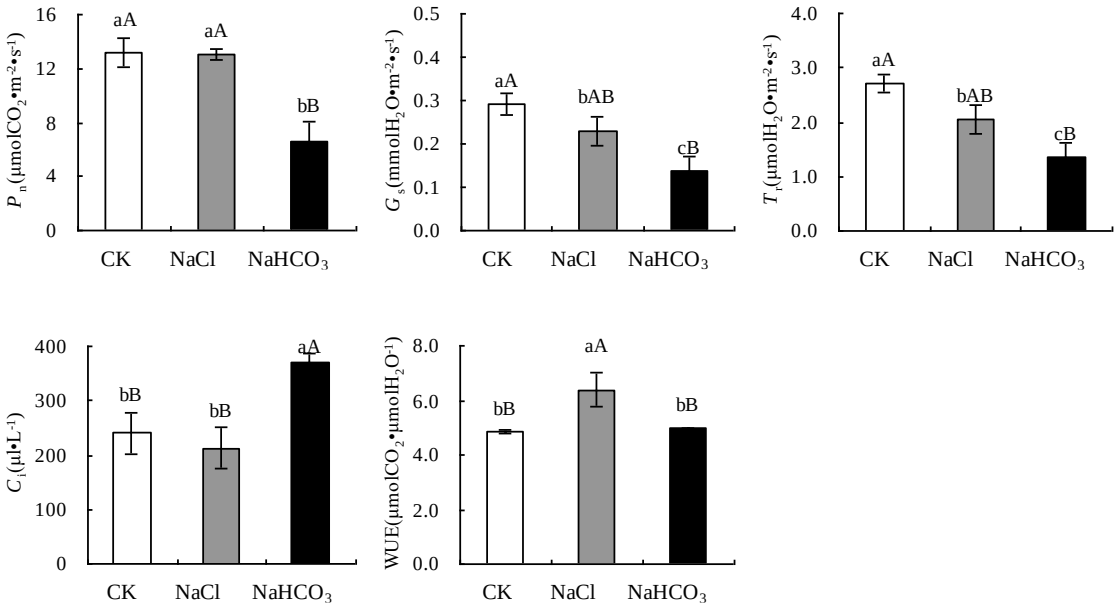

Fig. 5 Photosynthetic gas exchange parameters in leaves of mulberry seedlings under NaCl and $NaHCO_3$ stress.

A: net photosynthesis (P_n); B: stomatal conductance (G_s); C: transpiration rate (T_r); D: intercellular CO_2 concentration (C_i); E: water use efficiency (WUE)

Note: significant differences were expressed by different small letters (P<0.05), and very significant differences were expressed by different capital letters (P<0.01).

Tab. 4 Expression of proteins related to dark reactions in leaves of mulberry seedlings under NaCl and $NaHCO_3$ stress

Protein accession	Protein description	Species	Gene name	MW [kDa]	Score	CK	T1	T2
R4I779	Ribulose bisphosphate carboxylase large chain (Fragment) (RbcL)	*Morus alba*	rbcL	21.136	-2	1.18±0.04aA	1.10±0.05aA	0.80±0.07bB
O20258	Ribulose bisphosphate carboxylase large chain (Fragment) (RbcL)	*Morus alba*	rbcL	47.59	3.9659	1.20±0.05aA	1.25±0.03aA	0.66±0.04bB
Q32625	Ribulose bisphosphate carboxylase large chain (Fragment) (RbcL)	*Morus rubra*	rbcL	51.606	323.31	1.14±0.02aA	1.15±0.03aA	0.77±0.01bB
U3GQJ9	Ribulose bisphosphate carboxylase large chain (Fragment) (RbcL)	*Morus alba*	rbcL	27.577	12.559	1.10±0.08aA	1.18±0.05aA	0.80±0.02bB
W9RUU9	Ribulose bisphosphate carboxylase small chain (RbcM)	*Morus notabilis*	L484_014647	20.456	260.34	1.18±0.01aA	1.20±0.01aA	0.70±0.01bB
A8QIH7	Ribulose-1,5-bisphosphate carboxylase/oxygenase activase (RCA)	*Morus alba*	-	27.191	90.557	1.27±0.06aA	1.22±0.01aA	0.59±0.05bB
W9S2F0	Ribulose bisphosphate carboxylase/oxygenase activase 1 (RCA1)	*Morus notabilis*	L484_025296	51.766	323.31	1.23±0.11aA	1.23±0.02aA	0.68±0.05bB
W9RCR8	Ribulose bisphosphate carboxylase/oxygenase activase 2 (RCA2)	*Morus notabilis*	L484_025354	48.001	323.31	1.20±0.05aA	1.19±0.06aA	0.69±0.02bB
W9S0A8	Ribulose-1,5 bisphosphate carboxylase/oxygenase large subunit N-methyltransferase (RBCMT)	*Morus notabilis*	L484_015694	56.271	42.805	1.02±0.03bB	1.25±0.07aA	0.80±0.04cC
W9QMR3	Ribulose-1,5 bisphosphate carboxylase/oxygenase large subunit N-methyltransferase (RBCMT)	*Morus notabilis*	L484_004862	60.12	5.0452	1.15±0.17aA	1.20±0.06aA	0.74±0.03bB
W9R524	Phosphoglycerate kinase (PGK)	*Morus notabilis*	L484_003011	49.857	323.31	1.09±0.02bB	1.19±0.02aA	0.78±0.02cC
W9QWX1	Phosphoglycerate kinase (PGK)	*Morus notabilis*	L484_003013	42.641	259.36	0.76±0.02cC	0.98±0.01bB	1.21±0.02aA
W9RTC6	Glyceraldehyde-3-phosphate dehydrogenase (GAPD)	*Morus notabilis*	L484_006727	36.917	42.81	0.82±0.13bB	0.71±0.06bB	1.32±0.06aA
A0A1S6PVK8	Glyceraldehyde-3-phosphate dehydrogenase (Fragment) (GAPD)	*Morus alba*	g3pdh	13.375	105.87	0.79±0.04bB	0.74±0.13bB	1.39±0.08aA
W9R0D7	Glyceraldehyde-3-phosphate dehydrogenase (GAPD)	*Morus notabilis*	L484_023933	46.995	136.86	0.63±0.05bB	0.62±0.03bB	1.64±0.06aA
W9R8N5	Glyceraldehyde-3-phosphate dehydrogenase (GAPD)	*Morus notabilis*	L484_007581	42.969	323.31	1.09±0.01aA	1.09±0.01aA	0.88±0.01bB
W9QWT8	Glyceraldehyde-3-phosphate dehydrogenase (GAPD)	*Morus notabilis*	L484_024833	147.9	323.31	1.20±0.02aA	1.17±0.01aA	0.72±0.03bB
W9R6S4	Triosephosphate isomerase (TPI)	*Morus notabilis*	L484_024951	34.549	323.31	1.13±0.02aA	1.13±0.02aA	0.82±0.01bB
W9REN5	Sedoheptulose-1,7-bisphosphatase (SBPase)	*Morus notabilis*	L484_016237	42.6	190.02	1.22±0.05aA	1.23±0.02aA	0.65±0.03bB
A8DUA7	Chloroplast sedoheptulose-1,7-bisphosphatase (SBPase)	*Morus alba*	-	42.509	2.9261	1.30±0.12aA	1.23±0.07aA	0.60±0.05bB
W9RGS5	Transketolase (TK)	*Morus notabilis*	L484_025582	80.305	323.31	1.23±0.04aA	1.17±0.02aA	0.69±0.02bB

Preprints (www.preprints.org) | NOT PEER-REVIEWED | Posted: 14 May 2019 doi:10.20944/preprints201905.0167.v1

W9RQW9	Putative ribose-5-phosphate isomerase (R5PI)	*Morus notabilis*	L484_024593	30.793	85.756	0.77±0.06cC	1.27±0.01aA	0.99±0.01bB

Note: significant differences were expressed by different small letters (P<0.05), and very significant differences were expressed by different capital letters (P<0.01).

2.5 Photoprotection related proteins in leaves of mulberry seedlings under NaCl and $NaHCO_3$ stress

Under NaCl stress, q_P was slightly lower than CK and this difference was not significant (Fig. 6). NPQ increased by 12.76% (P<0.05), while (1-q_P)/NPQ and CK had no significant difference. Under $NaHCO_3$ stress, q_P and NPQ decreased by 37.80% (P<0.01) and 49.32% (P<0.01) compared with CK, respectively, but (1-q_P)/NPQ increased by 174.36% (P<0.01).

Under NaCl stress (Fig. 7), the A+Z content increased by 108.33% (P<0.01), while under $NaHCO_3$ stress, its content decreased by 27.08% (P<0.05). The content of V+A+Z did not change significantly under NaCl and $NaHCO_3$ stress. The proportion of (A+Z)/(V+A+Z) under NaCl stress increased by 62.73% (P<0.01), but that under $NaHCO_3$ stress decreased by 41.04% (P<0.01).

The results in Tab. 5 revealed that VDE expression increased by 14.57% (P<0.01) and ZE expression decreased by 7.65% (P<0.01) compared with CK under NaCl stress. The expression of VDE and ZE decreased very significantly under $NaHCO_3$ stress. The difference in expression between ndhN expression and CK was not significant, but the expression of ndhH, ndhI, ndhK, and ndhM increased by 20.33% (P<0.01), 11.59% (P<0.05), 22.50% (P<0.01), and 43.10% (P<0.01) in the CEF pathway under NaCl stress, respectively. However, their expression decreased very significantly under $NaHCO_3$ stress. In addition, the expression of Fd-GOGAT and Fd-GOGAT2 decreased significantly under NaCl stress compared with CK, but the reduction of their expression under $NaHCO_3$ stress was much greater than that under NaCl stress. Compared with CK, the expression of FTR (W9SEM5 and W9RQM9) under NaCl stress increased by 39.23% (P<0.01) and 7.95% (P<0.05), respectively. In addition, Fd-NiR expression increased by 9.96% (P<0.05), but the expression of FTR and Fd-NiR under $NaHCO_3$ stress decreased very significantly.

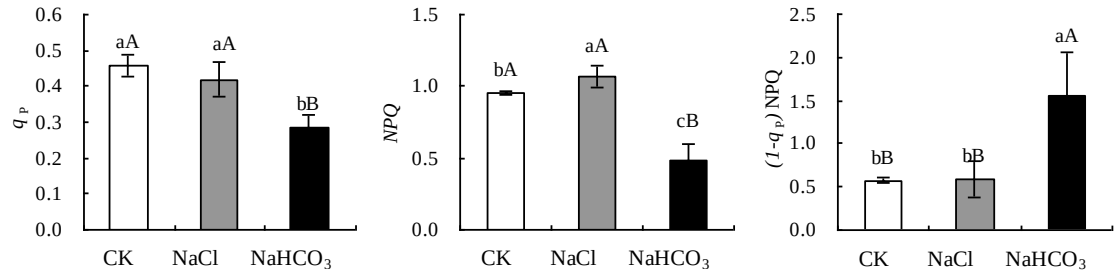

Fig. 6 The q_P (A), NPQ (B), and (1-q_P)/NPQ (C) in leaves of mulberry seedlings under NaCl and $NaHCO_3$ stress

Note: significant differences were expressed by different small letters (P<0.05), and very significant differences were expressed by different capital letters (P<0.01).

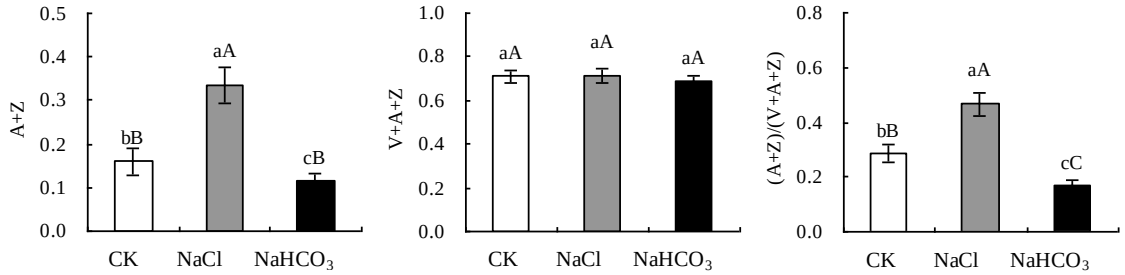

Fig. 7 Effects of NaCl and $NaHCO_3$ stress on the xanthophyll cycle in leaves of mulberry seedlings

A: A+Z; B:V+A+Z; C:(A+Z)/ (V+A+Z)

Note: significant differences were expressed by different small letters (P<0.05), and very significant differences were expressed by different capital letters (P<0.01).

Tab. 5 Expression of proteins related to photoprotective mechanism in leaves of mulberry seedlings under NaCl and $NaHCO_3$ stress

Protein	Protein description	Species	Gene name	MW	Score

accession				[kDa]		CK	T1	T2
W9S244	Violaxanthin de-epoxidase (VDE)	*Morus notabilis*	L484_006461	57.655	169.69	1.16±0.05bB	1.33±0.04aA	0.84±0.01cC
A0A0A0QZ09	Zeaxanthin epoxidase (ZE)	*Morus alba* var. multicaulis	-	73.917	164.07	1.11±0.01aA	1.07±0.02bA	0.88±0.02cB
Q09WW2	NAD(P)H-quinone oxidoreductase subunit H (ndhH)	*Morus indica*	ndhH	45.575	18.594	1.02±0.03bB	1.23±0.03aA	0.85±0.02cC
W9QPC3	NAD(P)H-quinone oxidoreductase subunit I (ndhI)	*Morus notabilis*	ndhI	16.503	22.016	1.09±0.07bA	1.22±0.08aA	0.79±0.02cC
Q09X13	NAD(P)H-quinone oxidoreductase subunit K (ndhK)	*Morus indica*	ndhK	25.397	15.352	1.02±0.03bB	1.25±0.06aA	0.83±0.05bB
W9QMA9	NAD(P)H-quinone oxidoreductase subunit M (ndhM)	*Morus notabilis*	ndhM	24.748	88.293	0.92±0.09aA	1.32±0.05aA	0.82±0.04bB
W9RKW4	NAD(P)H-quinone oxidoreductase subunit N (ndhN)	*Morus notabilis*	ndhN	25.438	15.122	1.20±0.05aA	1.17±0.02bB	0.72±0.05cC
W9SAH2	Ferredoxin-dependent glutamate synthase (Fd-GOGAT)	*Morus notabilis*	L484_01938	116.28	323.31	1.25±0.01aA	1.17±0.01bB	0.66±0.02cC
W9RZU3	Ferredoxin-dependent glutamate synthase 2(Fd-GOGAT2)	*Morus notabilis*	L484_019389	61.555	323.31	1.26±0.02aA	1.18±0.02bB	0.66±0.02cC
W9SEM5	Ferredoxin-thioredoxin reductase (FTR)	*Morus notabilis*	L484_003491	16.254	111.15	1.03±0.03bB	1.44±0.03aA	0.64±0.05cC
W9RQM9	Ferredoxin-thioredoxin reductase (FTR)	*Morus notabilis*	L484_011027	18.452	9.8583	1.17±0.05bA	1.26±0.06aA	0.66±0.04cB
W9RY59	Ferredoxin--nitrite reductase(Fd-NiR)	*Morus notabilis*	L484_027526	65.212	5.8264	1.11±0.08bA	1.23±0.09aA	0.75±0.02cB
W9RCI8	Glutamate--glyoxylate aminotransferase (GGAT)	*Morus notabilis*	L484_027698	53.503	323.31	1.08±0.01bB	1.15±0.01aA	0.85±0.01cC
W9QW05	Serine--glyoxylate aminotransferase (SGAT)	*Morus notabilis*	L484_002102	39.642	323.31	0.75±0.04bB	1.47±0.04aA	0.82±0.01bB

Note: significant differences were expressed by different small letters (P<0.05), and very significant differences were expressed by different capital letters (P<0.01).

3. Discussion

3.1 Response of photosynthesis and related proteins of leaves of *M. alba* seedlings to NaCl and $NaHCO_3$ stress

Chlorophyll fluorescence technology plays an important role in analyzing the absorption and utilization of light energy in photosynthesis. The effects of salt stress on plant PS II function are related to plant species, salt concentration, and treatment time (Everard et al., 1994; Lu et al., 2003). In this experiment, F_v/F_m, PI_{ABS}, and PI_{total}, which characterize the photochemical activity of PSII in *M. alba* seedlings, were not significantly different from CK under NaCl stress (100 mmol·L^{-1}), but significantly decreased under $NaHCO_3$ stress (100 mmol·L^{-1}). This indicated that PSII photochemical activity had a strong tolerance to NaCl stress, while the same concentration of alkaline $NaHCO_3$ stress significantly reduced the PSII activity of leaves of *M. alba*. PSII sites that were damaged under NaCl and $NaHCO_3$ stress were analyzed using the fast chlorophyll fluorescence induction curve (OJIP) in this study. The results showed that under NaCl stress, V_J on the standardized O-P curve and V_K on the standardized O-J curve did not vary significantly, but V_J and V_K increased significantly under $NaHCO_3$ stress. V_J can reflect the accumulation of Q_A^-, i.e., the enhancement of V_J indicates that the electron transfer from Q_A to Q_B on the PSII receptor side is blocked (Haldimann et al., 1999; Zhang et al., 2016a), and the increase of V_K is considered a specific marker of damage to OEC activity of the PSII electron donor side (Zhang et al., 2012b; Zhang et al., 2018b). Therefore, the results in this study indicate that there was no significant effect of NaCl stress on electron transport in the PSII donor side and receptor side of *M. alba* seedlings. Studies conducted by Lu (2003) and Askari (2010) also reported that NaCl stress had no significant effect on the PSII activities of *Suaeda salsa* and *S. aegyptiaca*. Under $NaHCO_3$ stress, the reasons for the decrease of photochemical activity of PSII in *M. alba* seedlings and the hindrance of the electron transfer rate are directly related to the hindrance of electron transfer at the donor side and receptor side of PSII.

To further analyze the intrinsic causes of PSII function changes under NaCl and $NaHCO_3$ stress, proteomic techniques were used to study the changes of protein expression in PSII protein complexes of mulberry seedlings. The PSII protein complex in advanced plants consists of 25 large subunits, such as the light-harvesting complex (LHCII), oxygen evolution complex (OEC), peripheral antenna complex, and the core proteins of D1 and D2 (Nishiyama et al., 2011). In terms of the donor side of PSII, it was found that the OEC activity and protein expression were significantly affected by salt stress (Abbasi Komatsu, 2004; Park et al., 2004). Allakhverdiev *et al.* (2001) reported that NaCl treatment (500 mmol·L^{-1}) led to irreversible inactivation of OEC in *Synechococcus*, and studies by Kim (2005), Abbasi (2004), and Chen (2009) demonstrated that OEC-related protein expression was up-regulated under NaCl stress. In this experiment, under NaCl stress, the expression of OEE1 and OEE2 on the donor side of PSII

decreased significantly, but the expression of OEE 3-1 and PPD4 increased significantly, while the expression of PsbP-like protein 1 and PPD3 did not change significantly, which indicates that the effects of NaCl stress on the PSII donor-side related proteins are inconsistent. Combined with the changes of V_K, it can be concluded that NaCl stress does not significantly affect the OEC function on the PSII donor side. The core of the OEC is the combination of Mn cluster in Ca^{2+} and Cl^-, so Cl^- plays an important role in stabilizing OEC functions. In this study, the activity of OEC on the donor side of PSII did not decrease significantly under NaCl stress, which may be related to the role of Cl^- (Pang et al., 2010; Zhang et al., 2016b). However, under $NaHCO_3$ stress, except for the significant increase of PPD4 expression, the expressions of other related proteins in the PSII donor side were significantly decreased compared with CK. The V_K of mulberry seedlings was also significantly increased under $NaHCO_3$ stress, which suggests that $NaHCO_3$ stress causes severe damage to OEC on the donor side of PSII. On the PSII receptor side, the expression of D1, D2, PsbE, and PBH did not change significantly under NaCl stress, but the expression of these proteins reduced significantly under $NaHCO_3$ stress. Combined with the results of the changes of V_J, it can be concluded that 100 $mmol \cdot L^{-1}$ NaCl stress does not cause the degradation of electron transfer related proteins in the PSII receptor side, but the reduction of protein expression under $NaHCO_3$ stress hinders the electron transfer in the PSII receptor side.

The main functions of CP43 and CP47 proteins are to receive excitation energy transmitted from peripheral antenna pigment complex of CP24, CP26, and CP29, and to transfer excitation energy to the pigment protein complexes in the reaction center (Casazza et al., 2010; Zhang et al., 2010). It is also necessary for photosynthetic oxygen evolution (Putnam-Evans et al., 1997; Vermaas et al., 1993). Shu *et al.* (2012) found that CP47 protein in cucumber seedling leaves decreased significantly under salt stress, but there was little effect on CP43 protein. However, other reports demonstrate that CP47 protein increased significantly under salt stress (Sengupta et al., 2009; Pang et al., 2010). In this experiment, CP47 decreased significantly under NaCl stress and CP43 did not change significantly. Under $NaHCO_3$ stress, the expression of CP43 and CP47 protein both decreased significantly, which is one of the important reasons for the reduction of photosynthetic oxygen evolution capacity and electron transfer rate in *M. alba* seedlings under $NaHCO_3$ stress. In addition, if CP43 and CP47 proteins cannot effectively receive excitation energy from peripheral antenna proteins, excess excitation energy will induce the production of ROS, such as singlet oxygen, and lead to oxidative damage to the photosynthetic mechanism.

PSI is also one of the action sites of stress (Bu et al., 2009; Zhang et al., 2009). During red light irradiation, the relative difference ($\triangle I/I_o$) of 820 nm optical signal is considered as an index reflecting the activity of PSI (Zhang et al., 2018c). In this experiment, the $\triangle I/I_o$ of *M. alba* seedlings under NaCl stress was significantly higher than CK, while that under NaHCO stress significantly decreased. In addition, the expression of PsaA, PsaB, PsaC, PsaD, and psaE decreased significantly under NaCl stress, but that of PsaF, PsaG, PsaH, PsaL, PsaN, and Ycf4 increased to varying degrees. Up-regulation of protein expression may play an important role in enhancing PSI activity of *M. alba* seedlings under NaCl stress, especially the up-regulation of Ycf4 protein expression, which showed great influence to the assembly of PSI and its stable attachment to the thylakoid membrane (Krech et al., 2012). The studies conducted by Takizawa (2009), Wang (2009), and Shikanai (2007) also suggested that NaCl stress increased PSI activity in algae and rice, which is similar to the results of Sudhir *et al.* (2005). However, the expression of the above proteins was significantly down-regulated under $NaHCO_3$ stress. The $\triangle I/I_o$, that is, the PSI of leaves of *M. alba* seedlings is more sensitive to $NaHCO_3$ stress, but the activity of PSI was relatively enhanced under NaCl treatment.

In addition to PSII and PSI complexes, PQ, Cyt b6f complex, PC, Fd, and FNR are also involved in the linear electron transfer process of photosynthesis. The down-regulation of the expression of proteins related to the linear electron transfer process affects the formation of ATP and NADPH (Wei et al., 2011; Caruso et al., 2008). Studies have shown that salt stress significantly affected the expression of Cyt_{b6} complex-related proteins(Zörb et al., 2009; Xu et al., 2010; Sobhanian et al., 2010). In this experiment, except for the up-regulation of petB expression and no significant change of PC, the expression of petA, PetC, Fd, and FNR decreased significantly under NaCl stress, but the expression of these electron transfer related proteins decreased significantly under $NaHCO_3$ stress. The decreased expression of these proteins was much greater in under $NaHCO_3$ stress than that under NaCl stress. Salt stress can lead to degradation of protein subunits on plant ATP synthase and inhibit ATP synthesis (Bandehagh et al., 2011; Sobhanian et al., 2010). However, the results in this study showed that the expression of atpA and atpB in *M. alba* seedlings increased significantly under NaCl stress, but decreased significantly under $NaHCO_3$ stress. The up-regulation of the expression of ATP synthase related subunits under NaCl stress may play an important role in reducing the electronic pressure. PSII and PSI

complexes and electron transport-related proteins perform their functions by attaching to thylakoid membranes. Under stress, the structure of thylakoid membranes is damaged or the membranes become dissociated, which directly leads to the shedding of attached proteins, thereby affecting the electron transfer function. In this study, V_L on the standardized O-K curve did not change significantly under NaCl stress, but it increased significantly under $NaHCO_3$ stress (Fig. 1 and Fig. 2). The increase of V_L is considered to be an important marker of changes in thylakoid membrane fluidity and destruction of its functional and structural integrity (Essemine et al., 2012; Tóth et al., 2005). Therefore, the reason for the decrease of PSII and PSI photochemical activity in *M. alba* seedlings and the hindrance of electron transport are related to the damage of the thylakoid membrane caused by $NaHCO_3$ with its higher pH. The changes of proteins related to the photoreaction process of *M. alba* seedlings under NaCl and $NaHCO_3$ stress are shown in Fig. 8.

Under NaCl stress, G_s in *M. alba* seedlings decreased with the reduction of T_r, but P_n and C_i did not decrease significantly, which led to a significant increase in WUE. Under $NaHCO_3$ stress, P_n, G_s, and T_r decreased significantly, and the reduction was much greater than that under NaCl stress, in addition to the increase of C_i. According to the criteria by Farquhar and Sharkey (1982), it is believed that the effect of NaCl stress on the photosynthetic function of *M. alba* is mainly reflected in stomatal factors, and the improvement of WUE in *M. alba* seedlings through the reduction of G_s also plays an important role. Under $NaHCO_3$ stress, photosynthesis was mainly restricted by non-stomatal factors. Yang *et al.* (2008) also found that alkaline salts had greater effects on the photosynthetic function of *Cleris virgata* than neutral salts. Among non-stomatal factors, Calvin cycle-related enzymes are important limiting factors, and many studies have shown that the expression of Calvin cycle-related enzymes is significantly affected by salt stress (Liska et al., 2004). Yu *et al.* (2011 and 2013) reported that the expression of RuBisCO protein in leaves of *Puccinellia tenuiflora* was significantly down-regulated under salt or alkali stress, while that of halophyte *Tamarix hispid* was significantly up-regulated under $NaHCO_3$ stress (Gao et al., 2008). In this experiment, the key enzymes, rbcL, rbcM, RCA, RCA1, RCA2, and RBCMT (W9QMR3), related to Rubisco carbon assimilation showed little change under NaCl stress, and RBCMT (W9S0A8) even significantly increased. However, the expression of these enzymes and their related subunits were significantly decreased under $NaHCO_3$ stress. The CO_2 fixation in the dark reactions is mainly restricted by carboxylation of RuBP and regeneration of RuBP. In this experiment, the differential proteins PGK (W9R524 and W9QWX1) and R5PI identified during the regeneration of RuBP were significantly up-regulated under NaCl stress. GAPD, TPI, SBPase, and TK did not change significantly, and the key enzyme, SBPase, in glucose synthesis did also not change significantly. This indicated that NaCl stress promoted the regeneration of RuBP and the synthesis of glucose in *M. alba* seedlings during dark reactions, and it had little effect on the expression of key enzymes or the up-regulation of expression; no down-regulation was identified. However, except for the up-regulated expressions of PGK (W9QWX1), GAPD (W9RTC6, A0A1S6PVK8 and W9R0D7), and R5PI (W9RQW9), the expression of other proteins was significantly decreased under $NaHCO_3$ stress, which was a reason for the significant increase of C_i under $NaHCO_3$ stress. A study conducted by Wei *et al.* (2012) indicated that the down-regulation of RuBisCO expression in *S. corniculata* leaves under $NaHCO_3$ stress was an important reason for the decrease of CO_2 fixation and the increase of C_i. Restricted regeneration of RuBP is mainly related to insufficient supply of ATP and NADPH (Yamori et al., 2011; Raines et al., 2010). Therefore, the effect of $NaHCO_3$ stress on RuBP regeneration and glucose synthesis in the dark reactions of leaves was significantly greater than that of NaCl stress. The expression of key enzymes in the dark reactions was significantly reduced under $NaHCO_3$ stress, and the photoresponse was inhibited, which resulted in insufficient supply of assimilate. The changes of proteins related to the dark reactions in *M. alba* seedlings under NaCl and $NaHCO_3$ stress are shown in Fig. 9.

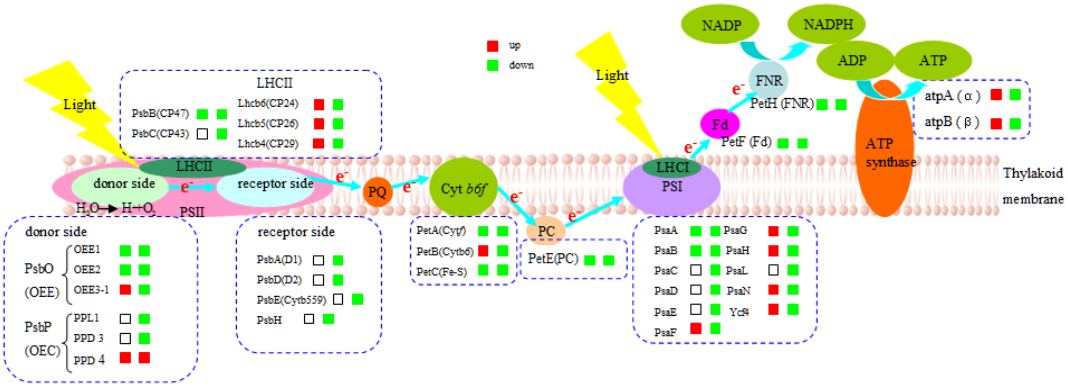

Fig. 8 Schematic presentation of NaCl and $NaHCO_3$ stress-responsive proteins involved in light reactions in *M. alba* seedlings.

Note: PSII: photosystem II, donor side: photosystem II electron donor side, receptor side: photosystem II electron receptor side, LHCII: light harvesting pigment protein complexe II, PsbB (CP47): photosystem II CP47 reaction center protein, PsbC (CP43): photosystem II CP43 reaction center protein, Lhcb6 (CP24): chlorophyll a-b binding protein CP24, Lhcb5 (CP26): chlorophyll a-b binding protein CP26, Lhcb4 (CP29): chlorophyll a-b binding protein CP29, , PsbO (OEE): oxygen-evolving enhancer protein, OEE1: oxygen-evolving enhancer protein 1, OEE2: oxygen-evolving enhancer protein 2, OEE3-1: oxygen-evolving enhancer protein 3-1, PPL1: PsbP-like protein 1, PPD3: PsbP domain-containing protein 3, PPD4: PsbP domain-containing protein 4, PsaA (D1): photosystem II D1 protein, PsbD (D2): photosystem II D2 protein, PsbE(Cytb559): cytochrome b559 subunit alpha, PsbH: photosystem II reaction center protein H, PQ: plastoquinone, Cyt*b6f*: cytochrome *b6f*, PetA (Cyt*f*): cytochrome *f*, PetB (Cyt*b6*): cytochrome *b6*, PetC (Fe-S): cytochrome b6-f complex iron-sulfur subunit, PetE (PC): plastocyanin, PSI: photosystem I, LHCI: light harvesting pigment protein complexe I, PsaA: photosystem I P700 chlorophyll a apoprotein A1, PsaB: photosystem I P700 chlorophyll a apoprotein A2, PsaC: photosystem I iron-sulfur center, PsaD: photosystem I reaction center subunit II, PsaE: photosystem I psaE, PsaF: photosystem I reaction center subunit III, PsaG: photosystem I reaction center subunit V, PsaH: photosystem I reaction center subunit VI, PsaL: photosystem I reaction center subunit XI, PsaN: photosystem I reaction center subunit N, ycf4: photosystem I assembly protein Ycf4, PetF (Fd): ferredoxin, PetH (FNR): ferredoxin--NADP reductase, atPA (α): ATP synthase subunit alpha, atpB (β): ATP synthase subunit beta.

The expression of related proteins are under NaCl and $NaHCO_3$ treatments from left to right. Red represents up-regulated protein expression, and green indicates for down-regulated expression.

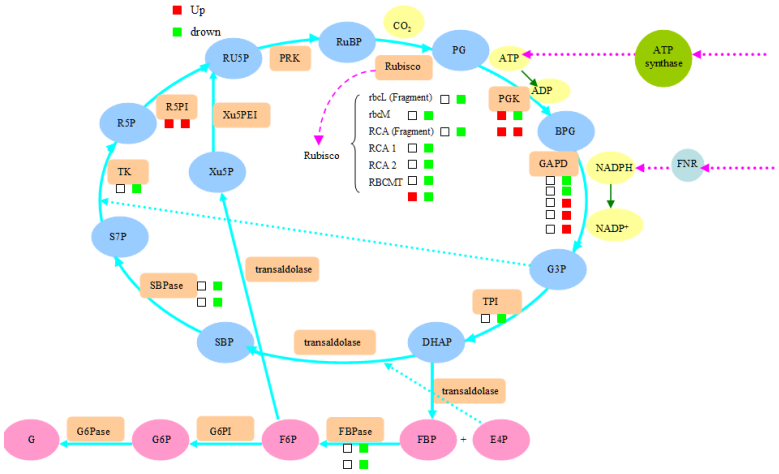

Fig.9 Schematic presentation of NaCl and $NaHCO_3$ stress-responsive proteins involved in the dark reactions (Glucose synthesis and RuBP regeneration) in *Morus alba* L. seedlings.

Note: RUBP: ribulose-1,5-bisphosphate, Rubisco: ribulose-1,5 bisphosphate carboxylase/oxygenase, rbcL(Fragment): Ribulose bisphosphatecarboxylase large chain (Fragment), rbcM: Ribulose bisphosphate carboxylase small chain, RCA (Fragment): ribulose-1,5 bisphosphate carboxylase/oxygenase activase (Fragment), RCA1: ribulose-1,5 bisphosphate carboxylase/oxygenase activase 1, RCA2: ribulose-1,5 bisphosphate carboxylase/oxygenase activase 2, RCBMT: ribulose-1,5 bisphosphate carboxylase/oxygenase large subunit N-methyltransferase, PG: 2,3-phosphoglycerate, ATP: adenosine triphosphate, ADP: adenosine diphosphate; PGK: phosphoglycerate kinase, BPG: 1,3-phosphoglycerate, GAPD: glyceraldehyde-3-phosphate dehydrogenase, NADPH: reduced nicotinamide adenine dinucleotide phosphate, $NADP^+$: oxidation nicotinamide adenine dinucleotide phosphate, G3P: glyceraldehyde 3-phosphate, TPI: triosephosphate isomerase, DHAP: dihydroxyacetone phosphate, SBP: sedoheptulose-1,7-bisphosphate, SBPase: sedoheptulose-1,7-bisphosphatase, S7P:

sedoheptulose7-phosphate, TK: transketolase, R5P: ribose 5-phosphate, R5PI: ribose-5-phosphate isomerase, Xu5P: D-xylulose 5-phosphate, Xu5PEI: D-xylulose 5-phosphate epimerase, Ru5P: ribulose-5-phosphate, PRK: ribulose-5-bisphosphate kinase, FBP: fructose-1,6 diphosphate, E4P: erythrose 4-phosphate, FBPase: fructose-1,6 diphosphatase, F6P: fructose-6 phosphate, G6PI: fructose-6 phosphate imerase, G6P: glucose -6 phosphate, G6Pase: glucose -6 phosphatase, G: glucose.

The expression of related proteins are under NaCl and $NaHCO_3$ treatments from left to right. Red represents up-regulated protein expression, and green indicates for down-regulated expression.

3.2 Response of photoprotective mechanism and related proteins of *Morus alba* L. seedlings to NaCl and $NaHCO_3$ stress

Cyclic electron flow (CEF) around PSI is an important photoprotective mechanism (Johnson, 2011; Miyake, 2010; Takahashi et al., 2009). The CEF pathway includes two main pathways, one involving NAD(P)H dehydrogenase NDH and the other involving the proton gradient regulatory protein PGR5. CEF also needs Cytb6f, PC, and PSI. Some studies have found that stress can induce the expression of NDH protein subunits and promote CEF processes (Lehtimäki et al., 2010; Bernhard et al., 2000). In this experiment, except for the not significant change in ndhN expression, the expression of ndhH, ndhI, ndhK, and ndhM were all significantly increased under NaCl stress; the expression of petB was also significantly increased. The expression of the above proteins was significantly decreased under $NaHCO_3$ stress. This indicated that CEF was enhanced under NaCl stress, but this protective mechanism was inhibited under $NaHCO_3$ stress. In addition to driving ATP synthase to synthesize ATP, the transthylakoid membrane proton gradient (△pH) produced by CEF plays an important role in protecting PSII and PSI (Ohnishi et al., 2005; Wang et al., 2006). Therefore, the reason for insignificant influence of PSII activity and significant increase of PSI activity under NaCl stress in this experiment may be related to the promotion of CEF processes, which is similar to the results of Hakala *et al.* (2005) who found that CEF has protective effect on PSII oxygen-releasing complex. CEF is usually not stimulated under weak light, or relative linear electron transfer is maintained at a relatively low level (Miyake et al., 2005; Nandha et al., 2007; Huang et al., 2012). However, when the ratio of NADPH/ATP is high, CEF is easily stimulated. For example, the increase of photorespiration leads to ATP consumption, or the CO_2 concentration in chloroplasts decreases and photorespiration increases as stomatal conductance decreases, resulting in more ATP supply than what is needed for CO_2 fixation, which leads to the increase of NADPH/ATP ratio and promotes CEF (Wang et al., 2006; Joët et al., 2000; Golding and Johnson, 2004). In this experiment, although G_s was significantly lower than CK under NaCl stress, the net photosynthetic rate (P_n) did not change. The utilization of ATP by leaves of *M. alba* seedlings under NaCl stress may increase, which may lead to the increase of the NADPH/ATP ratio, thus promoting CEF.

Under stress, if the electron transfer on the PSII electron transfer chain is blocked, the proton gradient (△pH) of the transthylakoid membrane can still be formed due to the continuous production of H^+ by PSII photolysis of H_2O in the thylakoid cavity. However, if △pH is not fully used to promote ATP production, the energy dissipation mechanism of the xanthophyll cycle depending on △pH will be activated. In addition, the △pH established by CEF will also drive the process of the xanthophyll cycle. The xanthophyll cycle exists in all advanced plants and some algae (Masojidek et al., 1999; Lohr et al., 2001). Studies have shown that the formation of A and Z in xanthophyll cyclic components is beneficial to dissipating excess excitation energy (Demmig-Adams, 1990), and the content of A and Z is positively correlated with energy dissipation(Eskling et al., 1997). Ruban *et al.* (1999) and Frank *et al.* (1994) found that Z could directly quench the excited state of chlorophyll *in vitro*, which indicated that the xanthophyll cycle is an important mechanism protecting the plant photosynthetic apparatus from excess light energy (Demmig-Adams and Adams, 1996). Salt stress can lead to the transformation of V to Z (Abadía et al., 1999), and it is reported that NPQ is positively correlated with heat dissipation dependent on the xanthophyll cycle (Kalituho et al., 2007; Li et al., 2000). Therefore, as an important way to dissipate excitation energy, NPQ plays an important role in reducing the pressure of the PSII reaction center and improving photosynthetic capacity of plants under stress (Johnson et al., 2007; Xu et al., 2018). In this study, under NaCl stress, NPQ increased compared with CK, excess light energy (1-q_P)/NPQ did not change significantly, and the expression of the key enzyme VDE in the xanthophyll cycle was up-regulated. However, ZE expression was down-regulated, resulting in a significant increase in the proportion of (A+Z)/(V+A+Z), which initiated the xanthophyll cycle to dissipate excess excitation energy. Han *et al.* (2010) demonstrated that overexpression of the VDE gene can effectively reduce the production of ROS in tomato leaves under low temperature stress to alleviate oxidative damage, and Qiu *et al.* (2003) also found that the anthophyll cycle plays an important role in improving salt

tolerance of *Atriplex centralasiatica*. In addition, it has been reported that the xanthophyll cycle exists in the antenna pigment protein complex of plant thylakoid membranes, and its pigments are mainly localized on LHCII and some small chlorophyll-binding proteins (CP24, CP26, and CP29) (Horton et al., 1996; Gilmore et al., 2010). CP24 and CP26 may also be one of the oxidases in the xanthophyll cycle (Schaller et al., 2011). In this study, the expression of the LHCII protein CP24 10A, CP26, and CP29 in PSII was up-regulated under NaCl stress (Tab. 1), which further demonstrated that the xanthophyll cycle played an important role in dissipating excess energy under NaCl stress, and the stability of the xanthophyll cycle was improved by enhancing the up-regulation of the xanthophyll cyclic attachment protein. Under $NaHCO_3$ stress, the expression of VDE and ZE in *M. alba* seedlings was down-regulated, and the proportion of (A+Z)/(V+A+Z) was also significantly reduced. The expression of CP24 10A, CP26, and CP29 also decreased. Therefore, the decrease of photochemical activity of PSII under $NaHCO_3$ stress was related to the inhibition of the xanthophyll cycle.

In addition to transferring electrons to FNR to promote the synthesis of ATP and NADPH, nitrogen metabolism, photorespiration, and ROS scavenging processes can also act as electron receptors for Fd. Some studies have found that these metabolic processes play a competitive role in the synthesis of NADPH, leading to a reduction in plant photosynthetic rate (Hu et al., 2014; Hu et al., 2015), but the absence of receptors for excess electrons in Fd can lead to the production of ROS around PSI under stress (Asada, 2006). Therefore, other electronic utilization pathways of Fd are also an important protective mechanism. In this experiment, the expression of Fd-FTR and Fd-NiR was significantly increased under NaCl stress. The proportion of electrons transferred to Fd used in nitrite reduction and the ROS scavenging metabolic pathway increased, which showed a positive effect on the reduction of ROS production caused by excess electrons. In addition, the results in this study also revealed that the expression of key enzymes (SGAT and GGAT) in photorespiration increased significantly, but the expression of Fd-GOGAT and Fd-GOGAT2 did not vary, which may imply that photorespiration has a positive effect on protecting the photosynthetic function of *M. alba* seedlings under NaCl stress. However, the expressions of Fd-GOGAT, Fd-GOGAT2, Fd-FTR, Fd-NiR, SGAT, and GGAT were significantly decreased under $NaHCO_3$ stress, which indicated that $NaHCO_3$ stress inhibited the other pathways of electron utilization, and the accumulation of excessive electrons in Fd inhibited photosynthetic linear electron transport, thus increasing the chance of ROS production. In addition, under $NaHCO_3$ stress, the reduction of NO_2^-, the assimilation of NH_4^+ during nitrogen metabolism in chloroplasts, and the expression of the key enzymes Fd-NiR, Fd-GOGAT, and Fd-GOGAT2 in photorespiration were all significantly reduced, which may lead to the accumulation of NO_2^- and NH_4^+ in chloroplasts and produce toxic effects. This may further inhibit the normal process of photosynthesis. The changes of proteins related to the photoprotective mechanism of *M. alba* seedlings under NaCl and $NaHCO_3$ stress are shown in Fig. 10.

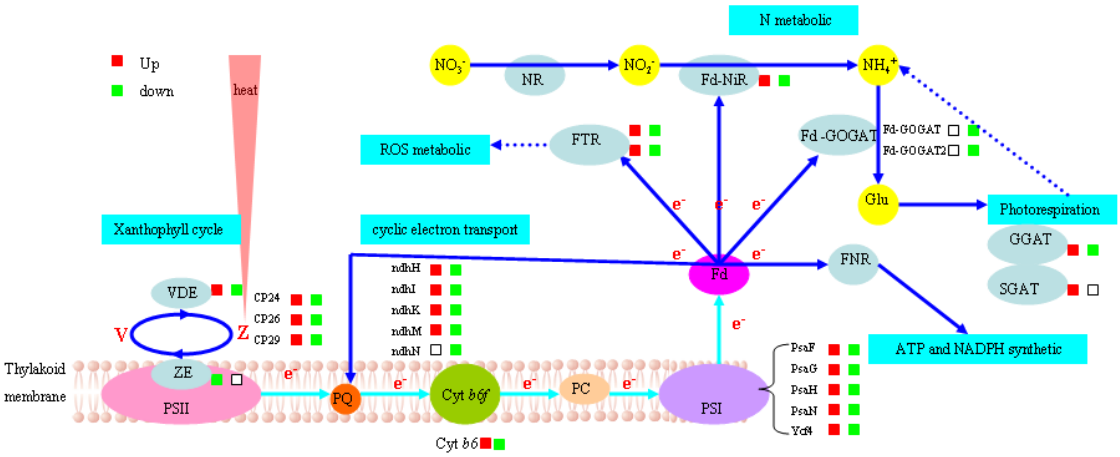

Fig.10 Schematic presentation of NaCl and $NaHCO_3$ stress-responsive proteins involved in photoprotective mechanism in *Morus alba* L. seedlings.

Note: Note: PSII: photosystem II, PQ: plastoquinone, Cyt*b6f*: cytochrome *b6f*, PC: plastocyanin, PSI: photosystem I, Fd: ferredoxin, FNR: ferredoxin--NADP reductase, V: Violaxanthin, Z: Zeaxanthin, VDE: violaxanthin de-epoxidase, ZE: zeaxanthin epoxidase, CP24: Chlorophyll a-b binding protein CP24, CP26: chlorophyll a-b binding protein CP26, ndhH: NAD(P)H-quinone oxidoreductase subunit H, ndhI: NAD(P)H-quinone oxidoreductase subunit I, ndhK: NAD(P)H-quinone oxidoreductase subunit K,ndhM: NAD(P)H-quinone oxidoreductase subunit M, ndhN: NAD(P)H-quinone oxidoreductase subunit E, PsaF: photosystem I reaction center subunit III, PsaG: photosystem I reaction center subunit V, PsaH: photosystem I reaction center subunit VI, PsaN: photosystem I reaction center subunit N, ycf4: photosystem I assembly protein Ycf4, FTR: ferredoxin-thioredoxin reductase, NR: nitrate reductase, Fd-NiR: ferredoxin--nitrite

reductase, Fd-GOGAT: ferredoxin-dependent glutamate synthase, Fd-GOGAT2: ferredoxin-dependent glutamate synthase 2, Glu: glutamate, GGAT: glutamate--glyoxylate aminotransferase, SGAT: serine--glyoxylate aminotransferase.

The expression of related proteins are under NaCl and $NaHCO_3$ treatments from left to right. Red represents up-regulated protein expression, and green indicates for down-regulated expression.

4. Conclusions

Under NaCl stress, the PSII activity of mulberry seedlings leaves was slightly affected, the PSI activity and the expression of some proteins on PSI increased to varying degrees, and the expression of subunits (atpA and atpB) in ATP synthase also increased significantly. However, this had little effect on the enzymes and proteins related to RuBP regeneration and glucose synthesis during dark reactions. However, under $NaHCO_3$ stress, the expression of proteins related to light and dark reactions identified in mulberry seedling leaves were mostly down-regulated, and photosynthetic electron transport and carbon assimilation were also significantly inhibited. In addition to stomatal factors, non-stomatal factors were the main limiting factors for inhibition of photosynthetic carbon assimilation.

CEF and the xanthophyll cycle play an important role in improving photosynthetic function of leaves of mulberry seedlings under NaCl stress. In other electronic utilization pathways of Fd, the expression of FTR and Fd-NiR increased significantly under NaCl stress, which could effectively reduce the electronic pressure on Fd. However, under $NaHCO_3$ stress, CEF, the xanthophyll cycle related proteins, and the expression of FTR, Fd-NiR, Fd-GOGAT, SGAT, and GGAT were all significantly down-regulated, destroying the photoprotective mechanism.

Acknowledgments: This research was supported by "Young Talents" Project of Northeast Agricultural University (18QC12; 18QC41) and The National Natural Science Fund (31500323; 31702282).

References:

Abadía A, Belkohodja R, Morales F, Abadía J. Effects of salinity on the photosynthetic pigment composition of barley (*Hordeum vulgare* L.) growth under a triple-line-source sprinkler system in the field. Journal of Plant Physiology, 1999,154(3): 392-400

Abbasi FM, Komatsu S. A proteomic approach to analyze salt-responsive proteins in rice leaf sheath. Proteomics, 2004, 4(7): 2072-81.

Akita S, Cabusla GS. Physiological basis of differential response to salinity in rice cultivars. Plant & Soil, 2000, 123(2): 277-294.

Allakhverdiev S I, Kinoshita M, Inaba M, Suzuki I, Murata N. Unsaturated fatty acids in membrane lipids protect the photosynthetic machinery against salt-induced damage in *Synechococcus*. Plant Physiology, 2001, 125(4): 1842-1853.

Asada K. Production and Scavenging of Reactive Oxygen Species in Chloroplasts and Their Functions. Plant Physiology, 2006, 141(2):391-396.

Askari H, Edqvist J, Hajheidari M, Kafi M, Salekdeh GH. Effects of salinity levels on proteome of *Suaeda aegyptiaca* leaves. Proteomics, 2010, 6(8): 2542-2554.

Bandehagh A, Salekdeh GH, Toorchi M, Mohammadi A, Komatsu S. Comparative proteomic analysis of canola leaves under salinity stress. Proteomics, 2011, 11(10): 1965-1975.

Bernhard TH, Lindberg MB, Vibe SH. Photoinhibition of Photosystem I in field-grown barley (*Hordeum vulgare* L.): Induction, recovery and acclimation. Photosynthesis Research, 2000, 64(1): 53-61.

Bhatnagar-Mathur P, Vadez V, Sharma KK. Transgenic approaches for abiotic stress tolerance in plants: retrospect and prospects. Plant Cell Reports, 2008, 27(3): 411-424.

Bu JW, Yao G, Gao HY, Jia YJ, Zhang LT, Cheng DD, Wang X. Inhibition mechanism of photosynthesis in cucumber leaves infected by *Sclerotinia sclerotiorum*(Lib.)de Bary. Acta Phytopatholgica Sinica,2009, 39(6): 613-621

Campbell SA, Nishio JN. Iron deficiency studies of sugar beet using an improved sodium bicarbonate-buffered hydroponic growth system. Journal of Plant Nutrition, 2000, 23(6): 741-757.

Caruso G, Cavaliere C, Guarino C, Gubbiotti R, Foglia P, Lagana A. Identification of changes in *Triticum durum* L. leaf proteome in response to salt stress by two-dimensional electrophoresis and MALDI-TOF mass spectrometry. Analytical & Bioanalytical

Chemistry, 2008, 391(1): 381-390.

Casazza AP, Szczepaniak M, Müller MG, Zucchelli G, Holzwarth AR. Energy transfer processes in the isolated core antenna complexes CP43 and CP47 of photosystem II. Biochimica et biophysica acta, 2010, 1797(9): 1606-1616.

Chao Y Y, Kao C H. Heat shock-induced ascorbic acid accumulation in leaves increases cadmium tolerance of rice (*Oryza sativa* L.) seedlings. Plant & Soil, 2010, 336(1-2):39-48.

Chen S, Gollop N, Heuer B. Proteomic analysis of salt-stressed tomato (*Solanum lycopersicum*) seedlings: effect of genotype and exogenous application of glycinebetaine. Journal of Experimental Botany, 2009, 60(7): 2005-2019.

Demmig-Adams B. Carotenoids and photoprotection in plants. A role for the xanthophyll zeaxanthin. Biochimica et Biophysica Acta (BBA) - Bioenergetics, 1990, 1020(1): 1-24

Demmig-Adams B, Adams WW. Xanthophyll cycle and light stress in nature: uniform response to excess direct sunlight among higher plant species. Planta, 1996, 198(3): 460-470.

Eskling M, Arvidsaon PO, Akerlund HE. The xanthophyll cycle, its regulation and components. Plant Physiology, 1997, 100(4): 806-816

Essemine J, Govindachary S, Ammar S, Bouzid S, Carpentier R. Enhanced sensitivity of the photosynthetic apparatus to heat stress in digalactosyl-diacylglycerol deficient *Arabidopsis*. Environmental & Experimental Botany, 2012, 80(3): 16-26.

Everard JD, Gucci R, Kann SC, Flore JA, Loescher WH. Gas exchange and carbon partitioning in the leaves of celery (*Apium graveolens* L.) at various levels of root zone salinity. Plant Physiology,1994,106:281-292.

Farquhar GD, Sharkey TD. Stomatal conductance and photosynthesis. Annual review of plant Physiology, 1982, 33(33): 317-345.

Forni C, Duca D, Glick B R. Mechanisms of plant response to salt and drought stress and their alteration by rhizobacteria. Plant & Soil, 2017, 410(1-2):335-356.

Frank HA, Cua A, Chynwat V, Young A, Gosztola D. Photophysics of the carotenoids associated with the xanthophyll cycle in photosynthesis. Photosynthesis Research, 1994,41(3):389-395.

Gao CQ, Wang YC, Liu GF, Yang CP, Jiang J, Li HY. Expression profiling of salinity-alkali stress responses by large-scale expressed sequence tag analysis in *Tamarix hispid*. Plant Molecular Biology, 2008, 66(3):245-258.

Gilmore AM. Mechanistic aspects of xanthophyll cycle-dependent photoprotection in higher plant chloroplasts and leaves. Physiologia Plantarum, 2010, 99(1):197-209.

Gilmore AM, Hazlett TL. Debrunner PG, Govindjee. Photosystem II chlorophyll a fluorescence lifetimes and intensity are independent of the antenna size differences between barley wild-type and chlorina mutants: Photochemical quenching and xanthophyll cycle-dependent nonphotochemical quenching of fluorescence. Photosynthesis Research, 1996, 4(1-2)8: 171-187

Greenway H, Munns R. Mechanisms of salt tolerance in nonhalophytes. Annual Review of Plant Physiology,1980, 31(4):149-190

Golding A J, Johnson G N. Down-regulation of linear and activation of cyclic electron transport during drought. Planta, 2004, 218(4):682-682.

Gong B, Wen D, Vandenlangenberg K, et al. Comparative effects of NaCl and $NaHCO_3$, stress on photosynthetic parameters, nutrient metabolism, and the antioxidant system in tomato leaves. Scientia Horticulturae, 2013, 157(3): 1-12.

Guo R, Yang ZZ, Li F, Yan CR, Zhong XL, Liu Q, Xia X, Li HR, Zhao L. Comparative metabolic responses and adaptive strategies of wheat (*Triticum aestivum*) to salt and alkali stress. BMC Plant Biology, 2015, 15(1):170.

Guan B, Yu JB, Lu ZH, Japhet W, Chen XB, Xie WJ. Salt tolerance in two *Suaeda* species: seed germination and physiological responses. Asian Journal of Plant Sciences, 2010,9:194-199

Guo R, Zhou J, Ren GX, Hao WP. Physiological responses of linseed seedlings to iso-osmotic polyethylene glycol, salt, and alkali stresses. Agronomy Journal, 2013,105(3): 764-772.

Haldimann P, Strasser R J. Effects of anaerobiosis as probed by the polyphasic chlorophyll a fluorescence rise kinetic in pea (*Pisum sativum* L.). Photosynthesis Research,1999,62(1):67-83

Han H, Gao S, Li B, Dong XC, Feng HL, Meng QW. Overexpression of violaxanthin de-epoxidase gene alleviates photoinhibition of PSII and PSI in tomato during high light and chilling stress. Journal of Plant Physiology, 2010, 167(3):176-183.

Hakala M, Tuominen I, Keränen M, Tyystjärvi T, Tyystjärvi E. Evidence for the role of the oxygen-evolving manganese complex in photoinhibition of Photosystem II. Biochimica et Biophysica Acta (BBA)- Bioenergetics, 2005, 1706(1): 68-80.

Horton P, And AVR, Walters R G. Regulation of light harvesting in green plants. Annual Review of Plant Physiology & Plant Molecular Biology, 1996, 47(1):655-684.

Hu YB, Sun GY, Wang XC. Induction characteristics and response of photosynthetic quantum conversion to changes in irradiance in mulberry plants. Journal of Plant Physiology, 2007, 164(8): 959-968.

Hu Y, Bellaloui N, Sun G, Tigabu M, Wang J. Exogenous sodium sulfide improves morphological and physiological responses of a hybrid *Populus* species to nitrogen dioxide. Journal of Plant Physiology, 2014, 171(10):868-875.

Hu Y, Bellaloui N, Tigabu M, Wang J, Diao J, Wang K, Yang R, Sun G. Gaseous NO_2 effects on stomatal behavior, photosynthesis and respiration of hybrid poplar leaves. Acta Physiologiae Plantarum, 2015, 37(2):1-8

Huang W, Yang S J, Zhang S B, Zhang JL, Cao KF. Cyclic electron flow plays an important role in photoprotection for the resurrection plant Paraboea rufescens under drought stress. Planta, 2012, 235(4):819-828.

Huang W, Yang YJ, Zhang SB. Specific roles of cyclic electron flow around photosystem I in photosynthetic regulation in immature and mature leaves. Journal of Plant Physiology, 2017,209(2):76-83

Huang W, Yang YJ, Zhang SB, Liu T. Cyclic electron flow around photosystem I promotes ATP synthesis possibly helping the rapid repair of photodamaged photosystem II at low light. Frontiers in Plant Science, 2018, 9: 239.

Johnson GN. Physiology of PSI cyclic electron transport in higher plants. Biochimica et Biophysica Acta-Bioenergetics, 2011, 1807(3): 384-389.

Johnson MP, Havaux M, Triantaphylidès C, Ksas B, Pascal AA, Robert B, Davison PA, Ruban AV, Horton P. Elevated zeaxanthin bound to oligomeric LHCII enhances the resistance of Arabidopsis to photooxidative stress by a lipid-protective, antioxidant mechanism. Journal of Biological Chemistry, 2007, 282(31):22605-22618

Joët T, Rumeau D, Cournac L, TA Kavanagh, Peltier G. Targeted inactivation of the plastid ndhB gene in tobacco results in an enhanced sensitivity of photosynthesis to moderate stomatal closure. Plant Physiology, 2000, 123(4):1337-1349.

Kalituho L, Beran K C, Jahns P. The transiently generated nonphotochemical quenching of excitation energy in arabidopsis leaves is modulated by zeaxanthin. Plant Physiology, 2007, 143(4):1861-1870.

Kim DW, Rakwal R, Agrawal GK, Jung YH, Shibato J, Jwa NS, Iwahashi Y, Iwahashi H, Kim DH, Shim Ie S, Usui K. A hydroponic rice seedling culture model system for investigating proteome of salt stress in rice leaf. Electrophoresis, 2005, 26 (23): 4521-4539.

Krech K, Ruf S, Masduki FF, Bednarczyk D, Albus CA, Tiller N, Hasse C, Schöttler MA, Bock R. The plastid genome-encoded Ycf4 protein functions as a nonessential assembly factor for photosystem I in higher plants. Plant Physiology, 2012, 159(2): 579-591.

Lehtimäki N, Lintala M, Allahverdiyeva Y, Aro EM, Mulo P. Drought stress-induced upregulation of components involved in ferredoxin-dependent cyclic electron transfer. Journal of Plant Physiology, 2010, 167(12): 1018-1022.

Li R, Shi F, Fukuda K. Interactive effects of various salt and alkali stresses on growth, organic solutes, and cation accumulation in a halophyte *Spartina alterniflora* (Poaceae). Environmental and Experimental Botany, 2010, 68(1): 66-74.

Li XP, Björkman O, Shih C, Grossman AR, Rosenquist M, Jansson S, Niyogi KK. A pigment- binding protein essential for regulation of photosynthetic light harvesting. Nature, 2000, 403: 391-395.

Liska AJ, Shevchenko A, Pick U, Katz A. Enhanced photosynthesis and redox energy production contribute to salinity tolerance in *Dunaliella* as revealed by homology-based proteomics. Plant Physiology, 2004, 136(1): 2806-2817.

Lohr M, Wilhelm C. Xanthophyll synthesis in diatoms: quantification of putative intermediates and comparison of pigment conversion kinetics with rate constants derived from a model.Planta,2001,212(3): 382-391.

Lu CM, Jiang GM, Wang BS, Kuang TY. Photosystem II photochemistry and photosynthetic pigment composition in salt-adapted halophyte *Artimisia anethifolia* grown under outdoor conditions. Journal of Plant Physiology,2003,160:403-408

Lu CM, Qiu NW, Wang BS, Zhang JH. Salinity treatment shows no effects on photosystem II photochemistry, but increases the resistance of photosystem II to heat stress in halophyte *Suaeda salsa*. Journal of Experimental Botany, 2003, 54(383): 851-860.

Masojidek J, Torzillo G, Koblized M, Kopecký J, Bernardini P, Sacchi A, Komenda J. Photoadaptation of two members of the Chlorophyta (Scenedesmus and Chlorella) in laboratory and outdoor cultures: changes in chlorophyll fluorescence quenching and the xanthophyll cycle. Planta,1999, 209(1):126-135.

Messant M, Timm S, Fantuzzi A, Weckwerth W, Bauwe H, Rutherford AW, Krieger-Liszkay A. Glycolate induces redox tuning of

photosystem II in vivo: study of a photorespiration mutant. Plant Physiology, 2018,177(3):1277-1285

Mitsuya S, Takeoka Y, Miyake H. Effects of sodium chloride on foliar ultrastructure of sweet potato (*Ipomoea batatas* Lam.) plantlets grown under light and dark conditions in vitro. Journal of Plant Physiology, 2000, 157(6): 661-667.

Miyake C. Alternative electron flows (water-water cycle and cyclic electron flow around PSI) in photosynthesis: molecular mechanisms and physiological functions. Plant & Cell Physiology, 2010, 51(12): 1951-63.

Miyake C, Miyata M, Shinzaki Y, Tomizawa K. CO_2 response of cyclic electron flow around PSI (CEF-PSI) in tobacco leaves--relative electron fluxes through PSI and PSII determine the magnitude of non-photochemical quenching (NPQ) of Chl fluorescence. Plant & Cell Physiology, 2005, 46(4):629-637.

Munns R, James RA. Approaches to increasing the salt tolerance of wheat and other cereals. Journal of Expermental Botany, 2006, 57(5): 1025-1043.

Nandha B, Finazzi G, Joliot P, Hald S, Johnson GN. The role of PGR5 in the redox poising of photosynthetic electron transport. Biochimica et Biophysica Acta (BBA) - Bioenergetics, 2007, 1767(10):1252-1259.

Nie ZJ, Hu CX, Sun XC, Tan QL, Liu HE. Effects of molybdenum on ascorbate-glutathione cycle metabolism in Chinese cabbage (*Brassica campestris* L. ssp. pekinensis). Plant & Soil, 2007, 295(1-2):13-21.

Nishiyama Y, Allakhverdiev SI, Murata N. Protein synthesis is the primary target of reactive oxygen species in the photoinhibition of photosystem II. Physiologia Plantarum, 2011, 142(1): 35-46.

Ohnishi N, Allakhverdiev SI, Takahashi S, Higashi S, Watanabe M, Nishiyama Y, Murata N. Two-step mechanism of photodamage to photosystem II: step 1 occurs at the oxygen-evolving complex and step 2 occurs at the photochemical reaction center. Biochemistry, 2005, 44(23): 8494-7499.

Oukarroum A, Goltsev V, Strasser RJ. Temperature effects on pea plants probed by simultaneous measurements of the kinetics of prompt fluorescence, delayed fluorescence and modulated 820 nm reflection. Plos One, 2013, 8: e59433.

Pang QY, Chen SX, Dai SJ, Chen YZ, Wang Y, Yan XF. Comparative proteomics of salt tolerance in *Arabidopsis thaliana* and *Thellungiella halophila*. Journal of Proteome Research, 2010, 9(5): 2584-2599.

Pang QY, Zhang AQ, Zang W, Wei L, Yan XF. Integrated proteomics and metabolomics for dissecting the mechanism of global responses to salt and alkali stress in Suaeda corniculata. Plant & Soil, 2016, 402(1-2):1-16.

Park CJ, Kim KJ, Shin R, Park JM, Shin YC, Paek KH. Pathogenesis-related protein 10 isolated from hot pepper functions as a ribonuclease in an antiviral pathway. Plant Journal, 2004, 37(2): 186-198.

Parida AK, Das AB. Salt tolerance and salinity effects on plants: a review. Ecotoxicology and Environmental Safety, 2005, 60(3): 324-349

Peng YL, Gao ZW, Gao Y, Liu GF, Sheng LX, Wang DL. Ecophysiological characteristics of alfalfa seedlings in response to various mixed saltalkaline stresses. Journal of Integrative Plant Biology, 2008, 50(1):29-39.

Pieters AJ, Tezara W, Herrera A. Operation of the xanthophyll cycle and degradation of D_1 protein in the inducible CAM plant, *Talinum triangulare*, under water deficit. Annals of Botany, 2003, 92(3): 393-399.

Putnam-Evans C, Bricker TM. Site-directed mutagenesis of the basic residues ^{321}K to ^{321}G in the CP 47 protein of photosystem II alters the chloride requirement for growth and oxygen-evolving activity in *Synechocystis* 6803. Plant Molecular Biology, 1997, 34(3): 455-463.

Qiu N, Lu Q, Lu C. Photosynthesis, photosystem II efficiency and the xanthophyll cycle in the salt‐adapted halophyte *Atriplex centralasiatica*. New Phytologist, 2003, 159(2):479-486.

Raines CA. Transgenic approaches to manipulate the environmental responses of the C3, carbon fixation cycle. Plant Cell & Environment, 2010, 29(3): 331-339.

Ruban AV, Johnson MP, Landrum JT, Wang XD, Wurtzel ET. Xanthophylls as modulators of membrane protein function. Archives of Biochemistry & Biophysics, 2010, 504(1):78-85.

Ruban AV, Horton P. The xanthophyll cycle modulates the kinetics of nonphotochemical energy dissipation in isolated light-harvesting complexes, intact chloroplasts, and leaves of spinach. Plant Physiology, 1999, 119(2): 531-542.

Sengupta S, Majumder AL. Insight into the salt tolerance factors of a wild halophytic rice, Porteresia coarctata: a physiological and proteomic approach. Planta, 2009, 229(4): 911-929.

Schaller S, Latowski D, Jemioła-Rzemińska M, Dawood A, Wilhelm C, Strzalka K, Goss R. Regulation of LHCII aggregation by different thylakoid membrane lipids. Biochimica et Biophysica Acta (BBA) - Bioenergetics, 2011, 1807(3):326-335.

Shikanai T. Cyclic electron transport around photosystem I: genetic approaches. Annual Review of Plant Biology, 2007, 58(1): 199-217.

Shu S. Study on phtotosynthetic mechanism of exogenous putrescine on alleviating salinity injury of cucumber seedlings. Nangjing Agricultural University. 2012.

Sobhanian H, Motamed N, Jazii FR, Nakamura T, Komatsu S. Salt stress induced differential proteome and metabolome response in the shoots of *Aeluropus lagopoides* (Poaceae), a halophyte C-4 plant. Journal of Proteome Research, 2010, 9(6): 2882-2897

Sobhanian H, Razavizadeh R, Nanjo Y, Ehsanpour AA, Jazii FR, Motamed N, Komatsu S. Proteome analysis of soybean leaves, hypocotyls and roots under salt stress. Proteome Science, 2010, 8(1): 19.

Song T, Xu H, Sun N, Jiang L, Tian P, Yong Y, Yang W, Cai H, Cui G. Metabolomic analysis of alfalfa (*Medicago sativa* L.) root-symbiotic rhizobia responses under alkali Stress. Frontiers in Plant Science, 2017, 8: 1208.

Strasser RJ, Srivastava A, Govindjee G. Polyphasic chlorophyll a fluorescence transient in plants and cyanobacteria. Photochemistry and Photobiology, 1995,61(1): 32-42

Sudhir PR, Pogoryelov D, Kovacs L, Garab G, Murthy SD. The effects of salt stress on photosynthetic electron transport and thylakoid membrane proteins in the cyanobacterium *Spirulina platensis*. Journal of Biochemistry Molecular Biology, 2005, 38(4): 481-485.

Sunil B, Saini D, Bapatla RB, Aswani V, Raghavendra AS. Photorespiration is complemented by cyclic electron flow and the alternative oxidase pathway to optimize photosynthesis and protect against abiotic stress. Photosynthesis Research, 2018:1-13.

Takizawa K, Takahashi S, Hüner NPA, Minagawa J. Salinity affects the photoacclimation of *Chlamydomonas raudensis* Ettl UWO241. Photosynthesis Research, 2009, 99(3): 195-203.

Takahashi S, Milward SE, Fan DY, Wahsoon C, Badger MR. How does cyclic electron flow alleviate photoinhibition in Arabidopsis?. Plant Physiology, 2009, 149(3): 1560-1567.

Tóth SZ, Schansker G, Kissimon J, Kovács L, Garab G, Strasser RJ. Biophysical studies of photosystem II-related recovery processes after a heat pulse in barley seedlings (*Hordeum vulgare* L.). Journal of Plant Physiology, 2005, 162(2): 181-194.

Vermaas WF, Styring S, Schröder WP, Andersson B. Photosynthetic water oxidation: The protein framework. Photosynthesis Research, 1993, 38(3): 249-263.

Wang P, Duan W, Takabayashi A, Endo T, Shikanai T, Ye JY, Mi H. Chloroplastic NAD(P)H dehydrogenase in tobacco leaves functions in alleviation of oxidative damage caused by temperature stress. Plant Physiology, 2006, 141(2): 465-474.

Wang RL, Hua C, Zhou F, Zhou QC. Effects of NaCl stress on photochemical activity and thylakoid membrane polypeptide composition of a salt-tolerant and a salt-sensitive rice cultivar. Photosynthetica, 2009, 47(1): 125-127.

Wei L, Zhang CY, Lu QT, Wen XG, Lu CM. The combined effect of salt stress and heat shock on proteome profiling in *Suaeda salsa*. Journal of Plant Physiology, 2011, 168(15): 1743-1752.

Wei L, Pang QY, Zhang AQ, Guo J, Yan XF. Effects of salt and alkali stresses on photosynthetic characteristics of *Suaeda corniculata* seedlings. Journal of Northeast Forestry University.2012, 40(1):32-35

Wu HF, Liu XL, You LP, Zhang LB, Zhou D, Feng JH, Zhao JM, Yu JB. Effects of salinity on metabolic profiles, gene expressions, and antioxidant enzymes in halophyte *Suaeda salsa*. Journal of Plant Growth Regulation, 2012, 31(3):332-341.

Xu CP, Sibicky T, Huang BR. Protein profile analysis of salt-responsive proteins in leaves and roots in two cultivars of creeping bentgrass differing in salinity tolerance. Plant Cell Reports, 2010, 29(6): 595-615.

Xu N, Zhang HH, Zhong HX, Wu YN, Li JB, Li X, Yin ZP, Zhu WX, Qu Y, Sun GY. The response of photosynthetic functions of F_1 cutting seedlings from *Physocarpus amurensis* Maxim (♀) × *Physocarpus opulifolius* “Diabolo” (♂) and the parental leaves to salt stress. Frontiers in Plant Science. 2018,9:714

Yan SH, Ji J, Wang G. Effects of salt stress on plants and the mechanism of salt tolerance.World Science-Technology Rearch& Development, 2006, 28(4): 70-76.

Yang C, Zhang ZS, Gao HY, Fan XL, Liu MJ, Li XD. The mechanism by which NaCl treatment alleviates PSI photoinhibition under chilling-light treatment. Journal of Photochemistry & Photobiology B Biology, 2014, 140:286-291.

Yamori W, Nagai T, Makino A. The rate-limiting step for CO_2 assimilation at different temperatures is influenced by the leaf nitrogen content in several C3 crop species. Plant Cell & Environment, 2011, 34(5): 764-777.

Yang CW, Chong JN, Li CY, Kim CM, Shi DC, Wang DL. Osmotic adjustment and ion balance traits of an alkali resistant halophyte Kochia sieversiana during adaptation to salt and alkali conditions. Plant & Soil, 2007, 294(1-2):263-276.

Yang CW, Jianar A, Li CY, Shi DC, Wang DL. Comparison of the effects of salt-stress and alkali-stress on photosynthesis and energy storage of an alkali-resistant halophyte *Chloris virgata*. Photosynthetica,2008, 46(2): 273-278.

Yu JJ, Chen SX, Zhao Q, Wang T, Yang CP, Diaz C, Sun GR, Dai SJ. Physiological and proteomic analysis of salinity tolerance in *Puccinellia tenuiflora*. Journal of Proteome Research, 2011, 10(9): 3852-70.

Yu JJ, Chen SX, Wang T, Sun GR, Dai SJ. Comparative proteomic analysis of *Puccinellia tenuiflora* leaves under Na_2CO_3 stress. International Journal of Molecular Sciences, 2013, 14(1):1740-1762.

Zhang AQ, Zang W, Zhang XY, Ma YY, Yan XF, Pang QY. Global proteomic mapping of alkali stress regulated molecular networks in *Helianthus tuberosus* L. Plant & Soil, 2016b, 409(1-2): 1-28

Zhang CM, Zou ZR, Huang Z, Zhang ZX. Effects of exogenous spermidine on photosynthesis of tomato seedlings under drought stress. Agricultural Research in the Arid Areas, 2010, 28(3): 182-187.

Zhang JT, Mu CS. Effects of saline and alkaline stress on the germination, growth, photosynthesis, ionic balance and anti-oxidant system in alkali-tolerant leguminous forage *Lathyrus quinquenervius*. Soil Science and Plant Nutrition, 2009, 55(5): 685-697.

Zhang HH, Zhang XL, Li X, Ding JN, Zhu WX, Qi F, Zhang T, Tian Y, Sun GY. Effects of NaCl and Na_2CO_3 stresses on the growth and photosynthesis characteristics of *Morus alba* seedlings. Chinese Journal of Applied Ecology, 2012a, 23(3): 625-631.

Zhang HH, Zhong HX, Wang JF, Sui X, Xu N. Adaptive changes in chlorophyll content and photosynthetic features to low light in *Physocarpus amurensis Maxim* and *Physocarpus opulifolius* "Diabolo". Peer J, 2016a, 4(3): 2125

Zhang HH, Xu N, Sui X, Long JH, Wu YN, Li JB, Wang JF, Qu Y, Sun GY. Arbuscular mycorrhizal fungi (*Glomus mosseae*) improves growth, photosynthesis and protects photosystem II in leaves of *Lolium perenne* L. under cadmium contaminated soil. Frontiers in Plant Science, 2018b, 9: 1156.

Zhang HH, Xu N, Wu XY, Wang JR, Ma SL, Li X, Sun GY. Effects of 4 kinds of sodium salt stress on plant growth, PS II and PS I function in leaves of Sorghum. Journal of Plant Interaction, 2018c, 13(1): 506-513.

Zhang MM, Fan DY, Sun GY, Chow WS. Optimising the linear electron transport rate measured by chlorophyll a fluorescence to empirically match the gross rate of oxygen evolution in white light: towards improved estimation of the cyclic electron flux around photosystem I in leaves. Functional Plant Biology, 2018a, 45:1138-1148

Zhang ZS, Li G, Gao HY, Zhang LT, Yang C, Meng QW. Characterization of Photosynthetic Performance during Senescence in Stay-Green and Quick-Leaf-Senescence, *Zea mays* L. Inbred Lines. Plos One, 2012b, 7(8): 42936

Zhang ZS, Zhang LT, Gao HY, Jia YJ, Bu JW, Meng QW. Research of the photoinhibition of PSI and PSII in leaves of cucumber under chilling stress combined with different light intensities. Scientia Agricultura Sinica,2009, 42(12): 4288-4293

Zhu JK. Plant salt tolerance. Trends in Plant Science, 2001, 6(2): 66-71.

Zörb C, Herbst R, Forreiter C, Schubert S. Short-term effects of salt exposure on the maize chloroplast protein pattern. Proteomics, 2009, 9(17): 4209-4220.